ผลของรีคอมบิแนนท์ไคเมอริกโปรตีนชนิดพีเคอาร์และเอพีเอเอฟ-1 ต่อการติดเชื้อไวรัสพีอาร์อาร์เอสในเซลล์ไลน์ เอ็มเออาร์ซี-145

นายวอ ฟอง วู อานห์ ตวัน

วิทยานิพนธ์นี้เป็นส่วนหนึ่งของการศึกษาตามหลักสูตรปริญญาวิทยาศาสตรดุษฎีบัณฑิต
สาขาวิชาอายุรศาสตร์สัตวแพทย์ ภาควิชาอายุรศาสตร์
คณะสัตวแพทยศาสตร์ จุฬาลงกรณ์มหาวิทยาลัย

ปีการศึกษา 2559

EFFECT OF RECOMBINANT CHIMERIC PKR-APAF-1 PROTEIN ON PRRS VIRUS INFECTED MARC-145 CELL LINE

Mr. Vo Phong Vu Anh Tuan

A Dissertation Submitted in Partial Fulfillment of the Requirements

for the Degree of Doctor of Philosophy Program in Veterinary Medicine

Department of Veterinary Medicine

Faculty of Veterinary Science

Chulalongkorn University

Academic Year 2016

Thesis Title	EFFECT OF RECOMBINANT CHIMERIC PKR-APAF-1 PROTEIN ON PRRS VIRUS INFECTED MARC-145 CELL LINE
By	Mr. Vo Phong Vu Anh Tuan
Field of Study	Veterinary Medicine
Thesis Advisor	Associate Professor Athipoo Nuntaprasert, D.V.M., Ph.D., D.T.B.V.M.
Thesis Co-Advisor	Associate Professor Achara Tawatsin, B.Sc., M.Sc.

Accepted by the Faculty of Veterinary Science, Chulalongkorn University in Partial Fulfillment of the Requirements for the Doctoral Degree

.....Dean of the Faculty of Veterinary Science

(Professor Roongroje Thanawongnuwech, D.V.M., M.Sc., Ph.D., D.T.B.V.P.)

THESIS COMMITTEE

.....Chairman

(Associate Professor Rosama Pusoonthornthum, D.V.M., M.Sc., Ph.D., D.T.B.V.M.)

.....Thesis Advisor

(Associate Professor Athipoo Nuntaprasert, D.V.M., Ph.D., D.T.B.V.M.)

.....Thesis Co-Advisor

(Associate Professor Achara Tawatsin, B.Sc., M.Sc.)

.....Examiner

(Associate Professor Meena Sarikaputi, D.V.M., M.Sc., Ph.D., D.T.B.V.M.)

.....Examiner

(Assistant Professor Nareerat Viseshakul, D.V.M., M.Sc., Ph.D.)

.....External Examiner

(Associate Professor Boonmee Sunyasootcharee, D.V.M., M.Sc.)

วอ ฟอง วู อานห์ ตวัน : ผลของรีคอมบิแนนท์ไคเมอริกโปรตีนชนิดพีเคอาร์และเอพีเอเอฟ-1 ต่อการติดเชื้อไวรัสพีอาร์อาร์เอสในเซลล์ไลน์ เอ็มเออาร์ซี-145 (EFFECT OF RECOMBINANT CHIMERIC PKR-APAF-1 PROTEIN ON PRRS VIRUS INFECTED MARC-145 CELL LINE) อ.ที่ปรึกษาวิทยานิพนธ์หลัก: อธิภู นันทประเสริฐ, อ.ที่ปรึกษาวิทยานิพนธ์ร่วม: อัจฉรา ธวัชสิน, 107 หน้า.

โรคสุกรไวรัส PRRS จัดเป็นเชื้อไวรัสที่สำคัญที่สุดและทำให้เกิดความสูญเสียทางเศรษฐกิจอย่างมหาศาลให้กับอุตสาหกรรมการเลี้ยงสุกรทั่วโลก แม้ว่าวิธีการมากมาย ที่จะนำไปใช้ในการควบคุม และป้องกันการเกิดโรคนี้ เช่น การฉีดวัคซีน และความปลอดภัยทางชีวภาพ การระบาดยังคงเกิดขึ้น ในการศึกษานี้ rcPAP ซึ่งสร้างขึ้นตามแนวคิด DRACO ใน มนุษย์ถูกสร้างขึ้น และผลิตโดยใช้ระบบ การแสดงออกของ ยีนผ่านเชื้อแบคทีเรียและศึกษาผลเหนี่ยวนำให้ เกิดภาวะ apoptosis ในเซลล์ไลน์ เอ็มเออาร์ซี-145 ที่ติดเชื้อไวรัส PRRS สายพันธุ์ US ที่แยกได้ ในประเทศไทย ในส่วนแรกของการศึกษา rcPAP ได้ถูกสร้าง ขึ้นด้วย 3 ส่วนประกอบ คือ ส่วนของโปรตีน ทีเอทีของเชื้อไวรัสเอชไอวี ซึ่งเป็นส่วนที่ใช้เจาะเข้าสู่เซลล์ ส่วนของโปรตีน PKR ที่ใช้ในการตรวจจับกับ dsRNA และส่วนของโปรตีน โดเมน CARD ของ Apaf-1 ที่ใช้เหนี่ยวนำให้เกิดภาวะ apoptotic โดย rcPAP ถูกผลิตโดย ใช้สองเวคเตอร์ ของระบบการแสดง ออกของยีน (PET-His6-TEV-LIC และ pQE32) และทำให้โปรตีนบริสุทธิ์จนเป็นเนื้อเดียวกัน ภายใต้เงื่อนไขตามธรรมชาติ โครงสร้างสามมิติ (3D) ของ rcPAP ถูกวิเคราะห์โดยใช้โปรแกรม I-TASSER (C-คะแนน = -4.27) พบว่า คล้ายกับโปรตีน PKR และ Apaf-1 ของมนุษย์ ซึ่งน่าจะมีการทำหน้าที่ที่คล้ายกัน rcPAP ที่ผลิตจากพลาสมิด His6-TEV-LIC เป็นโปรตีนที่ สามารถละลายน้ำ และได้ความเข้มข้นที่สูงกว่าพลาสมิด pQE32 ถึง 2.4 เท่า (12.32 มิลลิกรัมบริสุทธิ์ของ rcPAP ต่อลิตร) ที่อุณหภูมิต่ำ (25 ° C) สภาวะที่เหมาะสมสำหรับใช้ผลิต rcPAP คือ ความหนาแน่นของเชื้อแบคทีเรียที่ OD_{600} มีค่า 0.6 จะถูกเหนี่ยวนำด้วยสาร IPTG ที่ระดับ 0.75 mM อุณหภูมิ 25 องศาเซลเซียส เป็นเวลา 18 ชั่วโมง ในการศึกษาครั้งนี้ โพลีโคลนนอลแอนติบอดีต่อ rcPAP ได้ถูกผลิตขึ้น และตรวจยืนยัน การทำ ปฏิกิริยากับ rcPAP บริสุทธิ์โดยวิธี IFA และ indirect ELISA ในส่วนที่สองของการศึกษา เป็นการศึกษาผลของ rcPAP (ที่ความเข้มข้น 40, 60, 80 และ 120 ไมโครกรัม /มิลลิลิตร) ในหลอดทดลองที่มีผลต่อเซลล์ไลน์ เอ็มเออาร์ซี-145 หลังจากติดเชื้อไวรัส PRRS สายพันธุ์ US ที่แยกได้ในประเทศไทยเป็นเวลา 6 ชั่วโมง ต่อผลการเสริมประสิทธิภาพต้านไวรัส (เหนี่ยวนำให้เกิดภาวะ apoptotic เพื่อฆ่าเซลล์ที่ติดเชื้อไวรัส) ในชั่วโมงที่ 24, 48 และ 72 หลังการติดเชื้อ ผลการศึกษา พบว่า เซลล์ไลน์ เอ็มเออาร์ซี-145 ที่ได้รับโปรตีน rcPAP ที่ความเข้มข้น 40, 60 และ 80 ไมโครกรัม/มล ไม่เป็นพิษต่อเซลล์ โดยที่ความเข้มข้นของ rcPAP ที่ 80 ไมโครกรัม/มิลลิลิตร มีการเหนี่ยวนำให้เกิดภาวะ apoptotic สูงสุดและเพิ่มการต้านไวรัสในหลอดทดลองภายหลังการติดเชื้อไวรัสที่ 72 ชั่วโมง มีการเพิ่มระดับ caspase-3 อย่างมีนัยสำคัญ (16.09 เท่า (13.36 ± 0.003 VS 0.83 ± 0.003 ng/โปรตีน มก) ในเซลล์ไลน์ เอ็มเออาร์ซี-145 ที่ติดเชื้อไวรัส PRRS หลังจากได้รับโปรตีน rcPAP (80 ไมโครกรัม/มิลลิลิตร) เมื่อเทียบกับไม่ได้ รับโปรตีน จำนวนสำเนา RNA ของเชื้อไวรัส PRRS ได้ลดลงอย่างมีนัยสำคัญ 46.08% (3.86 ± 0.005 VS 7.16 ± 0.009 log10 (copies/ml)) ในเซลล์ และ 49.16% (3.34 ± 0.006 VS 6.57 ± 0.02 log10 copies/ml) ใน supernatants ของเซลล์ไลน์ เอ็มเออาร์ซี-145 ที่ได้รับโปรตีน rcPAP (80 ไมโครกรัม/มิลลิลิตร) เมื่อเทียบกับไม่ ได้รับโปรตีน ที่น่าสนใจ ไตเตอร์ของเชื้อไวรัสได้ลดลงอย่างมีนัยสำคัญ 67.9% (1.65 ± 0.003 VS 5.15 ± 0.01 log10 ($TCID_{50}$/ml)) ในเซลล์ไลน์ เอ็มเออาร์ซี-145 ที่ติดเชื้อไวรัส PRRS หลังจากได้รับโปรตีน rcPAP (80 ไมโครกรัม/มิลลิลิตร) เมื่อเทียบกับไม่ได้รับโปรตีน นอกจากนี้ ผลยังแสดงให้เห็นว่า rcPAP สามารถ ที่จะลดการสังเคราะห์ N โปรตีน ของเชื้อไวรัส PRRS และ การเกิดภาวะ CPE ในเซลล์ไลน์ เอ็มเออาร์ซี-145 ที่ติดเชื้อ สรุปผลจากการศึกษาครั้งนี้ ผู้วิจัยประสบความสำเร็จในการผลิต rcPAP และทำโปรตีนให้บริสุทธิ์ และแสดงให้เห็นว่า rcPAP สามารถเหนี่ยวนำให้เกิดการตายของเซลล์ไลน์ เอ็มเออาร์ซี-145 ที่ติดเชื้อไวรัส PRRS สายพันธุ์ US ได้ และเพิ่มกิจกรรมต้านไวรัสโดยการยับยั้งการแบ่งตัวของเชื้อไวรัส ผลการศึกษา ครั้งนี้ บ่งบอกว่า rcPAP มีแนวโน้มที่จะใช้เป็นสารต่อต้านการติดเชื้อไวรัส PRRS สายพันธุ์ US

ภาควิชา	อายุรศาสตร์	ลายมือชื่อนิสิต .....
สาขาวิชา	อายุรศาสตร์สัตวแพทย์	ลายมือชื่อ อ.ที่ปรึกษาหลัก .....
ปีการศึกษา	2559	ลายมือชื่อ อ.ที่ปรึกษาร่วม .....

5675503731 : MAJOR VETERINARY MEDICINE

KEYWORDS: ANTIVIRAL ACTIVITY / APOPTOSIS / MARC-145 CELL LINE / US STRAIN PRRS VIRUS / RCPAP

VO PHONG VU ANH TUAN: EFFECT OF RECOMBINANT CHIMERIC PKR-APAF-1 PROTEIN ON PRRS VIRUS INFECTED MARC-145 CELL LINE. ADVISOR: ASSOC. PROF. ATHIPOO NUNTAPRASERT, D.V.M., Ph.D., D.T.B.V.M., CO-ADVISOR: ASSOC. PROF. ACHARA TAWATSIN, B.Sc., M.Sc., 107 pp.

In swine disease, PRRS virus is recognized as the most significant viral pathogen and causes enormous economic losses to the swine industry worldwide. Although many methods are applied to control and prevent this disease, such as vaccination and biosecurity, outbreaks still occur. In this study, rcPAP that generated according to the human DRACO concept was constructed and produced using bacterial expression system and studied its apoptotic-induction effect on Thai isolated US strain PRRS virus-infected MARC-145 cells. In the first part, the rcPAP was constructed with 3 components of protein TAT HIV part as cell penetration, PKR part as dsRNA detection and CARD domain of Apaf-1 part as apoptotic induction. The rcPAP was produced using two different-expression systems (pET-His6-TEV-LIC and pQE32) and purified to apparent homogeneity under native conditions. The three-dimensional (3D) structure of rcPAP was predicted using I-TASSER software (C-score = -4.27) and was found to be similar to that of human PKR and Apaf-1 proteins, suggesting a similar respective function. The rcPAP produced from the pET-His6-TEV-LIC plasmid was expressed as a soluble protein at a 2.4-fold higher concentration (12.32 mg purified rcPAP per litre of culture) than those from the pQE32 plasmid at a low temperature (25 °C). The optimal condition for rcPAP production was found to be an inoculum cell density at an OD_{600} of 0.6 induced with 0.75 mM IPTG at 25 °C for 18 h. The mouse anti-rcPAP polyclonal antibodies were produced and found to successfully react with purified rcPAP by indirect immunofluorescence (IFA), western blot and indirect ELISA analyses. In the second part, the in vitro study of the rcPAP (at the concentration of 40, 60, 80 and 120 mg/ml) was studied to treat in MARC-145 cells after 6 h infected with Thai isolated US strain PRRS virus. The enhanced antiviral efficacy (apoptotic induction to kill virus-infected cells) was continued to determine at time course of 24, 48 and 72 hpi. The results demonstrated that rcPAP treated MARC-145 cells alone were no cytotoxicity at a concentration of 40, 60 and 80 mg/ml. The rcPAP concentration of 80 mg/ml at 72 hpi showed maximum apoptotic induction and enhanced antiviral activity in vitro. The rcPAP significantly increases the active caspase-3 levels (16.09 fold (13.36 ± 0.003 vs 0.83 ± 0.003 ng/mg protein) in PRRS virus-infected MARC-145 cells treated with rcPAP (80 mg/ml) when it was compared with no treatment. The PRRS viral RNA copy numbers were significantly reduced 46.08 % (3.86 ± 0.005 vs 7.16 ± 0.009 log10 (copies/ml)) in culture cells and 49.16 % (3.34 ± 0.006 vs 6.57 ± 0.02 log10 copies/ml) in culture supernatants of infected MARC-145 cells treated with rcPAP (80 mg/ml) when it was compared with no treatment. Interestingly, the viral titers were significantly reduced 67.9 % (1.65 ± 0.003 vs 5.15 ± 0.01 log10 ($TCID_{50}$/ml)) in Thai isolated US strain PRRS virus-infected MARC-145 cells treated with rcPAP (80 mg/ml) when it was compared with no treatment. In addition, the results also showed that the rcPAP was able to lower PRRS virus N protein synthesis and CPE in infected MARC-145 cells. In conclusion, the results from this study suggested that rcPAP successfully expressed, produced and purified and was induced apoptosis in US strain PRRS virus-infected MARC-145 cells and enhanced antiviral activity against virus replication. These results imply that the rcPAP is likely a valuable therapeutic agent against US strain PRRS virus infection.

Department:	Veterinary Medicine	Student's Signature	.....
Field of Study:	Veterinary Medicine	Advisor's Signature	.....
Academic Year:	2016	Co-Advisor's Signature	.....

ACKNOWLEDGEMENTS

The deepest appreciation goes to my primary mentor, Assoc. Prof. Dr. Athipoo Nuntaprasert, who has served as a father figure to me over the last three years and has given me the opportunity to achieve one of my scientific goals. I would like to thank Assoc. Prof. Achara Tawatsin for her invaluable encouragement, helpful suggestions and supervision throughout the course of this work.

I take this opportunity to express my deep sense of gratitude to the members of my Doctoral Scrutiny Committee Assoc. Prof. Dr. Rosama Pusoonthronthum, Assoc. Prof. Boonmee Sanyasootcharee, Assoc. Prof. Dr. Meena Sarikaputi and Assist. Prof. Dr. Nareerat Viseshakul for providing several suggestions and helpful guidance for improvement in research.

I would like to thank all lecturers and staffs of Department of veterinary medicine for their kind cooperation during my study.

I am indebted to my current and former Thai lab students for providing a stimulating and fun environment in which to learn and grow. I would like to thank my classmates and my friends in life.

This thesis would not be possible without full support from 'Scholarship for International Graduate Students in ASEAN Countries', Graduate School and Faculty of Veterinary Science, Chulalongkorn University. The financial and academic supports will contribute significantly to my future career and my life. I am always indebted for those.

Finally, I express my deepest gratitude to my dear parents and all my family members. I am eternally grateful for their everlasting support and faith in all my undertakings

CONTENTS

Page

Page

Page

List of tables

List of Figures

LIST OF ABBREVIATIONS

Apaf-1	=	Apoptotic Protease-Activating Factor-1
bp	=	base pair
BSA	=	Bovine serum albumin
CARD	=	Caspase recruitment domain
cDNA	=	Complementary DNA
CPE	=	Cytopathic effect
C-score	=	Confidence *score*
DCs	=	dendritic cells
DISC	=	Death-inducing signalling complex
DMEM	=	Dulbecco's modified Eagle's medium
DNA	=	deoxyribonucleic acid
dNTP	=	dATP, dGTP, dTTP, dCTP
DRACO	=	Double-stranded RNA (dsRNA) Activated Caspase Oligomerizer
dsRBD	=	dsRNA-binding domains
dsRBM	=	dsRNA binding motif
dsRNA	=	Double stranded ribonucleic acid
EDTA	=	Ethylenediaminetetraacetic acid
eIF2α	=	Eukaryotic translation initiation factor 2α
ELISA	=	enzyme-linked immunoassay
EU	=	European genotype
FMD	=	Foot and Mouth Disease
HIV	=	Human Immunodeficiency Virus
HP	=	High Pathogenic
HRP	=	Horseradish peroxidase
ICAD	=	Inhibitor of caspase activated DNAse
IFN	=	Interferon

IPMA	=	Immunoperoxidase Monolayer Assay
IPTG	=	Isopropyl-Beta-D-Thiogalactoside
I-TASSER	=	Iterative threading assembly refinement algorithm
LB	=	Luria Bertani
LV	=	Lelystad Virus
kDa	=	kilodalton
M	=	Protein marker
Met-tRNAi	=	Methionyl initiator transfer RNA
miRNAs	=	MicroRNAs
mRNA	=	Messenger ribonucleic acid
MTT	=	3-(4,5-Dimethylthiazol-2-Yl)-2,5-Diphenyltetrazolium Bromide
N protein	=	nucleocapsid protein
NOD	=	Nucleotide binding and oligomerization domain
OD	=	Optical density
ORFs	=	open reading frames
PAM	=	porcine alveolar macrophages
PBS	=	Phosphate buffered saline
PCR	=	polymerase chain reaction
PCV2	=	Porcine Circovirus type 2
PED	=	Porcine Epidemic Diarrhea
PKR	=	Protein kinase R
PMSF	=	Phenylmethanesulfonyl Fluoride
PRRS	=	porcine reproductive and respiratory syndrome
PVDF	=	Polyvinyl difluoride
qRT-PCR	=	Quantitative Real Time Reverse Transcriptase-Polymerase Chain Reaction;
rcPAP	=	Recombinant chimaeric swine PKR-Apaf-1 protein
RNA	=	Ribonucleic acid

rpm	=	Rounds per minute
RT-PCR	=	Reverse Transcriptase Polymerase chain reaction
SDS-PAGE	=	Sodium Dodecyl Sulfate Polyacrylamide Gel Electrophoresis
SiRNA	=	Small inhibitory RNA
TAT	=	Trans-activator transcription
$TCID_{50}$	=	50 % tissue culture infectious dose
TM-score	=	Traditional metrics score
US	=	North American genotype

General introduction

The porcine reproductive and respiratory syndrome (PRRS) is recognized as the most significant swine viral pathogens and causes economic losses worldwide (Neumann et al., 2005; Cho and Dee, 2006). This virus can infect swine only and currently no evidence showing that any other species is susceptible to PRRS virus infection (Van Breedam et al., 2013). Phylogenetic studies showed that PRRS virus has two main genotypes: the North American strain (US strain) is VR-2332 or type 2 and the European strain (EU strain) is the Lelystad Virus or type 1 (Meulenberg et al., 1997; Nelsen et al., 1998). Recently, the new PRRS virus strain, as China strain or highly pathogenic (HP) strain (related to type 2) is known for rapid and severe spread among Asian countries (Tian et al., 2009). The US strain PRRS virus is still greatly reported to cause abortion storm and respiratory disease complexes in pigs around the world (Karniychuk and Nauwynck, 2013). The high variability of various PRRS virus strains circulated in the farms make this virus remains hard to control. Although there has been extensive research on the control of these diseases, such as vaccination and the use of antiviral drugs or biosecurity, the disease still occurs. In general, the most effective method to control viral diseases is vaccination. The current use of PRRS modified live virus vaccines has not provided complete protection because of the viral virulence and this disease was often subsequently reoccurring in the pigs (Charerntantanakul, 2012).

MARC-145 cells derived from MA-104 monkey kidney cell line are important cell lines for studying the PRRS virus infection and show permission of the complete replication

cycle of PRRS virus and more convenient than the use of primary cells such as porcine alveolar macrophage (PAM) cells (Wensvoort et al., 1991; Bautista et al., 1993; Kim et al., 1993). Currently, many researches were reported the development of better and novel methods to control PRRS virus infection *in vitro*. For example, the interferon (IFN) is used as an important role to inhibit most of viral infections (Sang et al., 2010). The study of recombinant swine IFN-β on MARC-145 cells infected with US strain PRRS virus indicated that pre-treatment of MARC-145 cells with recombinant porcine IFN-β inhibited only US strain PRRS virus replication but not HP and EU strains (Overend et al., 2007). However, the licence to use this molecule has not been approved yet because of no any data from *in vivo* study. In another example, the study of Cecropin P1 (CP1) which is found in porcine intestine showed that this protein has not only revealed extracellular antiviral activity against PRRS virus, but also inhibited activity when administered either before, or after viral challenge in MARC-145 cells (Guo et al., 2014). The epigallocatechin gallate (EGCG) palmitate drug was studied for its activity to reduce PRRS viral infection in MARC-145 cells. This report indicated that anti-PRRS viral effects were considerably higher than that of EGCG or ribavirin when administered as a pre- or post-treatment. Moreover, the anti-PRRS viral effects of EGCG palmitate when administered before was more powerful than after or co-treatment (Zhao et al., 2014). However, EGCG palmitate was shown to be higher in cytotoxicity than the native EGCG. In addition, EGCG palmitate was suggested to add before PRRS virus infection. The last example of PRRS virus controlling method is

the use of antiviral drugs such as cidofovir or oseltamivir to control of swine viral diseases is limited compared with the use of antimicrobial agents because of various restricting factors such as adverse reaction, complexity, cost and resistance (Tempesta et al., 2007; Govorkova et al., 2009; Pozzo and Thiry, 2014).

There is an evidence suggesting a new variant strain of some swine viruses are resistant to antiviral drugs and that may become more powerful, such as super-viruses in human (Rider et al., 2011; Song et al., 2015; Zhou et al., 2015). Therefore, the new effective strategies to control swine viral diseases are urgently needed and will likely require utilizing the latest technologies and evolving practices to enhance the disease-fighting powers to eventually eradicate these viruses.

More recently, recombinant human DRACO molecule was developed for controlling virus-infected cells, including flaviviruses, bunyaviruses and influenza viruses (Rider et al., 2011). The human DRACO was constructed from the three different components: (1) the transduction peptide derived from the HIV TAT domain for entering cells, (2) a double stranded (ds) RNA recognition domain derived from human protein kinase R (PKR) (1–181 amino acids) for activation of the defensive interferon pathways, and (3) the caspase recruitment domain (CARD) of human Apaf-1 for inducing apoptotic caspase pathways (Rider et al., 2011). This molecule detects the long dsRNA helices of many viruses during their transcription and replication and induces rapid apoptosis selectively in enveloped or non-enveloped virus-infected cells but not in uninfected cells.

In 2015, there was a report showing the use of DRACO in pigs (Guo et al., 2015). This DRACO was synthesized based on the sequences of two natural cellular pathways and was constructed using swine PKR and human Apaf-1 instead of swine Apaf-1. The first process involved dsRNA detection using the two dsRNA-binding domains (dsRBD) of the swine PKR gene, while the apoptotic induction process was based the CARD domain of the human Apaf-1 gene (Guo et al., 2015). The DRACO in pigs exhibited antiviral activity against HP-PRRS virus infection by reducing viral RNA replication and protein production in both MARC-145 cells and in PAM. Moreover, the multiple alignments of the deduced amino acid sequences of the two dsRNA-binding domains of the swine PKR gene compared to those of other mammalian species are shown in Table 1.

Table 1 Comparison homology (%) of deduced amino acid sequences of the dsRBD of swine PKR and the CARD domain of swine Apaf-1 gene with those of other mammalian species

Sequences	Cattle	Mouse	Human
dsRBD of swine PKR	68.5 %	50 %	58.2 %
CARD domain of swine Apaf-1	92.7 %	85.5 %	87.6 %

The dsRBD of the swine PKR gene showed only 58.2 % deduced amino acid sequence similarity to the human PKR gene. The CARD domain of the swine Apaf-1 gene had the highest amino acid sequence homology to the bovine Apaf-1 gene and 87.6 %

sequence identity with the human Apaf-1 gene. Thus, the dsRBD of human PKR and the CARD domain of the human Apaf-1 gene might not have a specific function in pigs.

According to human DRACO concept, recombinant chimaeric swine PKR-Apaf-1 protein (rcPAP) was constructed comprising three parts: detection, apoptosis and delivery parts. The first part is the Trans-Activator transcription (TAT) protein which was used as protein transduction domain (PTD) derived from HIV TAT domain at the position of 47–57 amino acid sequences (GYARAAARQARAG) (Murriel and Dowdy, 2006). The second part is in the viral dsRNA detection pathway, the dsRBD derived from swine PKR. The swine PKR protein (Figure 1 A) comprises of an N-terminals with two dsRNA binding domains, a linker domain, and a C-terminal kinase domain. Swine PKR had two consensus motifs of the RNA-binding domain in the N-terminal region similar to those of other mammalian species (Asano et al., 2004). PKR is a latent Serine/Threonine kinase that is stimulated by binding to viral dsRNA synthesized during virus infection (Figure 1 B) (Samuel, 1993). Major natural PKR activators are produced in viral infected cells as by-components of viral replication or transcription. The viral dsRNA is made from viruses having a genome of positive-strand RNA, dsRNA, or DNA viruses. Nevertheless, dsRNA signals were not detected for RNA viruses with negative strand (Weber et al., 2006).

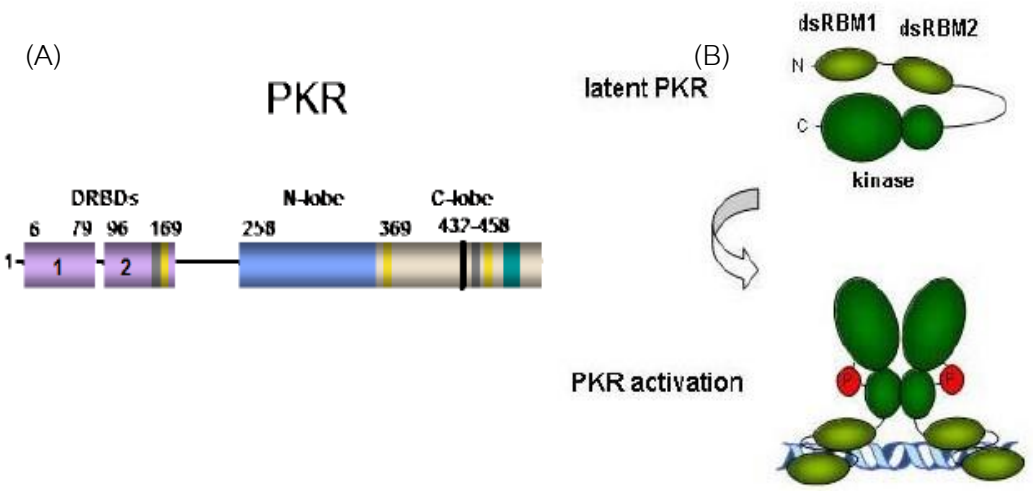

Figure 1. (A) Protein kinase R (PKR) and (B) Activation of PKR by viral dsRNA (Dauber and Wolff, 2009).

The third part is in the apoptotic induction pathway, the CARD domain of swine apoptotic protease-activating factor 1 (Apaf-1) was chosen. Swine Apaf-1 shown in Figure 2 contains three principal parts: the N-terminal caspase recruitment domain (CARD), the nucleotide binding and oligomerization domain (NOD), and the C-terminal regulatory WD40 repeat domain (Elmore, 2007). Apaf-1 belongs to intrinsic pathway of apoptosis, a causative apoptosis in the cell conducts the assembly of the apoptosome, which stimulates the initiator caspase-9. The activation of caspase-9 has been demonstrated using recombinant CARD domain of Apaf-1 and the CARD of Apaf-1 and caspase 9 is interactive by forming the complex in the proportion of 1:1 (Hu et al., 2014). Caspase-9 is an initiator caspase and exists as a latent monomeric type in the nonappearance of a stimulated apoptosis. The active caspase-9 activates effector caspase-3 by cleaving the

inhibitor of caspase activated DNAse (ICAD). Then, the effectors represent the execution level of the caspase cascade and conducts to apoptosis of the death cell. This activation pathway of caspase-3 results in DNA fragmentation, degradation of cytoskeletal and nuclear proteins, cross-linking of proteins, creation of apoptotic bodies, expression of ligands for phagocytic cell receptors and lastly uptake by phagocytic cells.

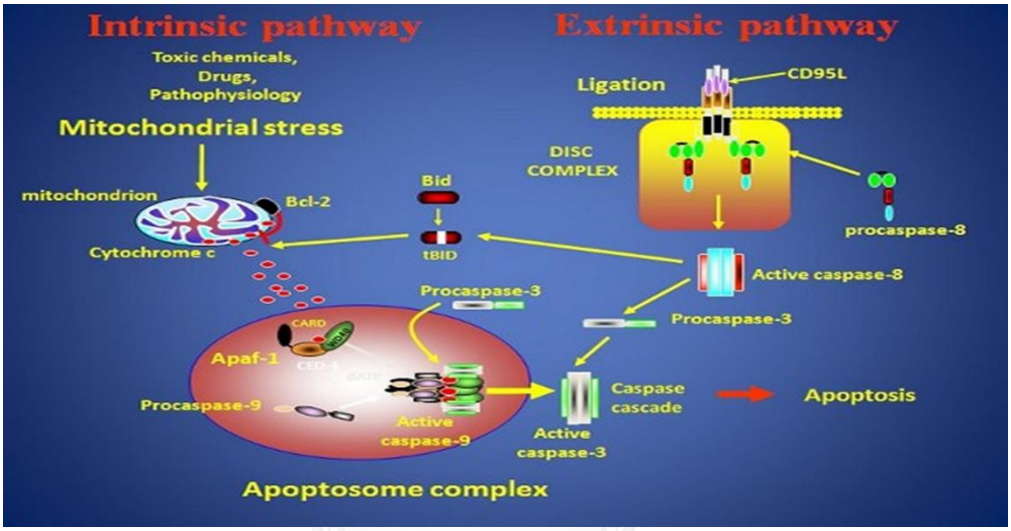

Figure 2. Schematic overview of the apoptotic pathways (Riedl and Salvesen, 2007)

A detail study on the production of rcPAP (Figure 3 A) with cloning, production and purification and the in vitro study of rcPAP with induction of apoptosis in virus-infected cell lines (Figure 3 B) including reduced effect on viral RNA copy numbers, viral titration, viral N protein synthesis and CPE may provide novel enhanced antiviral efficacy for use in controlling swine viral diseases. The main purposes of the present study are focuses on the production and the *in vitro* effect of rcPAP in MARC-145 cell line as follows:

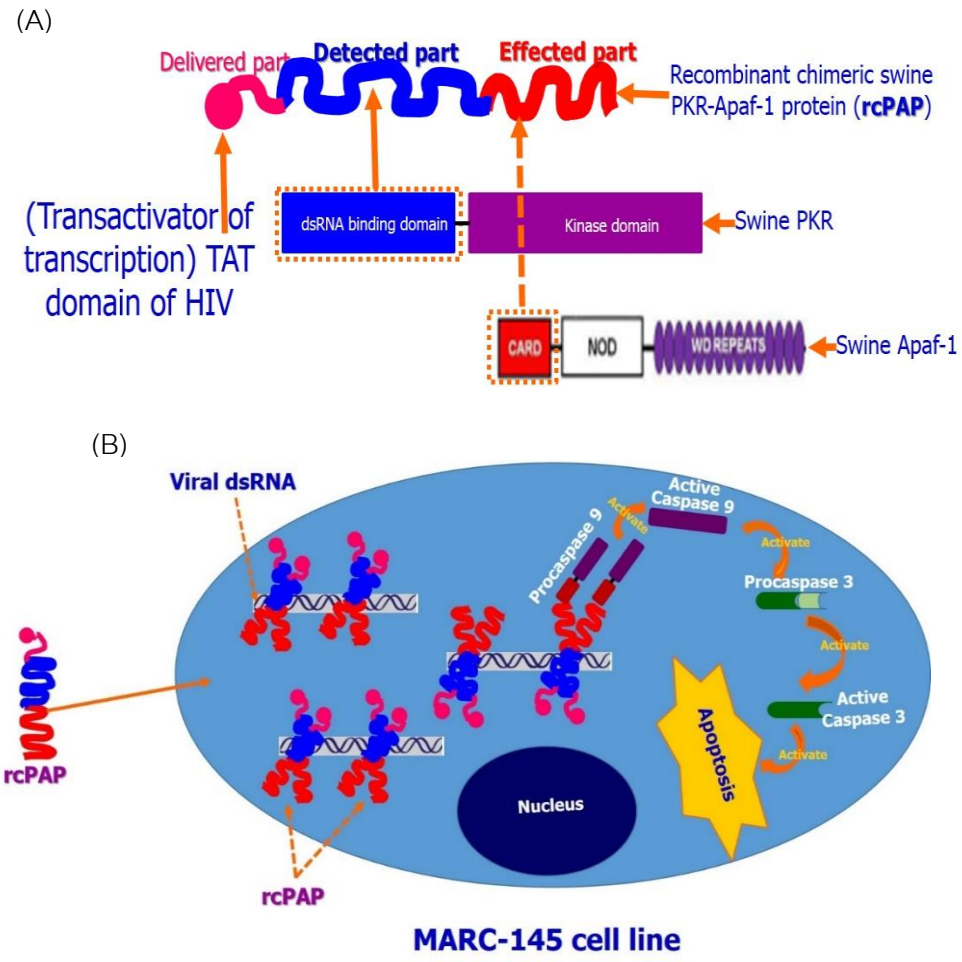

Figure 3. (A) Novel ideal structure of the rcPAP; (B) How rcPAP work to induce apoptosis in PRRS virus-infected MARC-145 cells.

In CHAPTER 1, the author described the molecular method to clone and produce the rcPAP using bacterial-expression system with two-different plasmids. In addition, the author compared the expression levels between two plasmids. Moreover, the author described the optimized condition for the production of rcPAP and also purification method. Furthermore, the author described the characterization of mouse specific

polyclonal antibodies reacted against rcPAP. The rcPAP was successfully produced and further use to perform *in vitro* study.

In CHAPTER 2, the author described the *in vitro* effect of rcPAP on Thai isolated US strain PRRS virus-infected MARC-145 cell line. Firstly, the author described the study of cytotoxicity of rcPAP on MARC-145 cell line. Secondly, the author described the penetration and persistence times of rcPAP in MARC-145 cells were determined. Finally, the rcPAP efficacy on the induction of apoptosis was measured, the reduction of viral RNA copy numbers, viral titration and the decreasing in viral N protein synthesis and CPE were also studied.

CHAPTER 1

Production of recombinant chimaeric swine PKR-APAF-1 proteins in a bacterial expression system

Abstract

The swine farms worldwide are at risk of viral disease infections, including porcine reproductive and respiratory syndrome (PRRS), classical swine fever, porcine epidemic diarrhoea and porcine circovirus type 2. Although many control and preventive methods are applied to these diseases, such as vaccination and biosecurity, outbreaks still occur. The use of recombinant chimaeric swine double-stranded RNA-dependent protein kinase (PKR)-apoptotic protease activator factor 1 (Apaf-1) proteins (rcPAP), which generated according to the human DRACO concept, is an alternative way to control viruses in swine. The rcPAP was constructed using Thai-isolated US strain PRRS virus-infected PAM, comprised of a delivery part (HIV TAT domain), a detector part (two dsRNA-binding domains of the porcine PKR gene) and an effector part (CARD domain of the porcine Apaf-1 gene). The rcPAP was expressed in *E. coli* using two different-expression systems (pET-His6-TEV-LIC and pQE32) and was enriched to apparent homogeneity under native conditions. The three-dimensional (3D) structure of rcPAP was predicted using I-TASSER software (C-score = -4.27) and was found to be similar to that of human PKR and Apaf-1 proteins, suggesting a similar respective function. The rcPAP produced from the pET-His6-TEV-LIC plasmid was expressed as a soluble protein at a 2.4-fold higher concentration (12.32 mg purified rcPAP/l of culture) than that from the pQE32 plasmid at a low temperature (25 °C). The optimal condition for the rcPAP production was found to be an inoculum cell density at an OD_{600} of 0.6 induced with 0.75 mM IPTG at 25 °C for 18

h. Mouse anti-rcPAP polyclonal antibodies were produced and found to successfully react with the rcPAP by indirect immunofluorescence, western blot and indirect ELISA analyses. This rcPAP is likely to be useful in controlling of PRRS viral infections in the future.

Keywords: Expression, Polyclonal antibody, Production, Purification, rcPAP, Soluble Protein.

Introduction

Swine farms are at risk to multiple serious and complicated viral diseases. Many of these viruses can survive in pig cells with long-term, chronic consequences, and most of them are difficult to treat because they are protected by the host's own cells. Porcine reproductive and respiratory syndrome (PRRS) with single stranded RNA of 15 Kb genome is one of the most prominent diseases in swine and causes adverse effects to the pig industry through both direct and indirect losses (Li et al., 2007). In addition, classical swine fever also causes important infectious diseases in pigs and wild boars, with significant economic losses in Asian countries (Dong et al., 2012). Porcine circovirus type 2 (PCV2) is the causative agent of PCV-associated disease while porcine endemic diarrhoea became an endemic disease in Asian pig farming countries with recent outbreaks in the United States in 2013 and in Canada and Mexico in 2014 (Sun et al., 2012; Seo et al., 2014; Vlasova et al., 2014; Song et al., 2015).

Although there has been extensive research on the control of these diseases, such as vaccination and the use of antiviral drugs or biosecurity, the diseases still occur. In general, the most effective method to control viral diseases is vaccination, but the current use of modified live PRRS virus vaccines has not provided complete protection, with viral virulence and disease often subsequently reoccurring in the pigs (Charerntantanakul, 2012). Moreover, the use of antiviral drugs for the control of swine viral diseases is limited

compared with the use of antimicrobial agents because of various restricting factors, such as adverse reaction, complexity, cost and resistance (Pozzo and Thiry, 2014).

Recently, recombinant human DRACO proteins were developed for controlling virus-infected cells, including flaviviruses, bunyaviruses and influenza viruses (Rider et al., 2011). The human DRACO was constructed from the three different components: (1) a double stranded (ds) RNA recognition domain derived from human protein kinase R (PKR) (1–181 amino acids) for activation of the defensive interferon pathways, (2) the caspase recruitment domain (CARD) of human Apaf-1 for inducing apoptotic caspase pathways, and (3) the transduction peptide derived from the HIV TAT domain for entering cells (Rider et al., 2011). This molecule detects the long dsRNA helices of many viruses during their transcription and replication and induces rapid apoptosis selectively in enveloped or non-enveloped virus-infected cells but not in uninfected cells. However, little information is available on the appropriate use of this type of recombinant chimaeric protein to reduce viral infections in veterinary medicine (Pozzo and Thiry, 2014).

In 2015, there is a report of the use of DRACO in pigs (Guo et al., 2015). This DRACO was synthesized based on sequences of two natural cellular pathways and it was constructed using swine PKR and human Apaf-1 instead of swine Apaf-1. The first process involved dsRNA detection using the two dsRNA-binding domains of the swine PKR gene, while the apoptotic induction process was based the CARD domain of the human Apaf-1 gene (Guo et al., 2015). The resultant DRACO exhibited antiviral activity

against highly pathogenic (HP)-PRRS virus infections by reducing viral RNA replication and protein production in both MARC-145 cells and in PAM. However, the two dsRNA-binding domains of the swine PKR gene showed only 58.2 % amino acid sequence similarity to the human PKR gene. The CARD domain of the swine Apaf-1 gene had the highest amino acid sequence homology to the bovine Apaf-1 gene (92 %) and 87.6 % sequence identity with the human Apaf-1 gene. Thus, the two dsRNA-binding domains of human PKR and the CARD domain of the human Apaf-1 gene might not have any specific functional activity in pigs.

To control the variant or super-viruses that occur in swine in the future, novel antiviral peptide molecules, such as the DRACO chimaeric molecule, that originate from a suitable swine host are urgently need. In general, the sequence alignments of the full-length swine PKR and Apaf-1 genes lack specificity. Taken together with previous reports, the dsRBD (two dsRNA-binding domains (dsRBD1 and dsRBD2)) of swine PKR and the CARD domain of swine Apaf-1 are viewed as better candidate peptides for a more specific study of viral dsRNA detection and apoptotic induction (Rider et al., 2011; Guo et al., 2015). In this study, a recombinant chimaera containing portions of the swine PKR and Apaf-1 genes was engineered from the cDNA of PAMs and a transducing tag with trans-activator transcription (TAT) protein. This chimaeric peptide may play an important role as a self-defence mechanism in pigs, resulting in the destruction of virus-infected cells by apoptosis. The objective of this study was to produce the recombinant chimaeric

swine PKR-Apaf-1 protein (rcPAP) in an *E. coli* expression system to be used as a potential candidate for the control of PRRS viral loads in pigs.

Materials and Methods

Bacterial strains and plasmid vectors

The pCR2.1 TA plasmid (Invitrogen, USA) was used to construct the TAT-PKR-Apaf-1 chimaera and was then transformed into *E. coli* strain DH5α (Invitrogen, USA). Two bacterial expression plasmids were constructed to express the rcPAP with an N-terminal $(His)_6$ tag: the pQE32 (QIAGEN, Germany) and the pET-His6-TEV-LIC plasmids (Addgene, USA). The pQE32 and the pET-His6-TEV-LIC plasmids were transformed into the M15 (pREP4) and BL21 (DE3) *E. coli* strains, respectively.

Expression of rcPAP

Cloning

The purified RT-PCR products encoding the dsRBD of porcine PKR (582 bp) (P) (GenBank Accession Number: **AB104654**) (Asano et al., 2004) and the CARD domain of porcine Apaf-1 (297 bp) (A) (GenBank Accession Number: **XM_003481742**) (Riedl et al., 2005) cDNA from US strain PRRS virus-infected PAMs were directly inserted in the pCR2.1®TA plasmid (Invitrogen, USA) after amplification using the primers shown in Table 2 and RT-PCR conditions in Table 3. The HIV TAT domain was added to the PKR forward primer (amino acid sequence: YGRKKRRQRRR) (Gump and Dowdy, 2007). The plasmids were named pCR2.1-P and pCR2.1-A and were propagated in the DH5α host cell. The digested fragment from pCR2.1-A was inserted into pCR2.1-P at the *AgeI* restriction site,

and the correct orientation of the pCR2.1-P-A plasmid was confirmed by PCR amplification and sequencing analyses. The sequences of the porcine PKR and the CARD domain of the porcine Apaf-1 cDNA were submitted to GenBank with accession numbers **KP729189** and **KP729186**, respectively.

Table 2 Nucleotide sequences of PCR primers used for RT-PCR

Gene	Sense	Sequence (5' to 3')	GenBank accession number	Product sizes (bp)
1. TAT-PKR RBD part	+	*CCCGGG*TATGGTCGTAAAAAGCGTCGT CAGCGTCGTCGTGCCAGTGGTCGTTCA	AB104654	582
	-	*ACCGGT*TCAGACTGTGCTTTTCACAGA		
2. Apaf-1 CARD part	+	*ACCGGT*GATGCAAAAGCTCGAAATTGT	XM_003481742	297
	-	*ACCGGTGTCGAC*GGAAGAAGAGACGA CAGG		
3. NSP 2 (full)	+	AAAGACCAGATGGAGGAGGA	GU454850	756
	-	GAGCTGAGTATTTTGGGCGTG		
4. NSP 2 (deleted)	+	AAAGACCAGATGGAGGAGGA	GU454850	666
	-	GAGCTGAGTATTTTGGGCGTG		
5. ORF 7	+	ATGCCAAATAACAACGGCAAG	GQ330474	478
	-	TCATGCTGAGGGTGATGCTGT		
6. TAT-PKR RBD-Apaf-1 CARD	+	*CCCGGG*TATGGTCGTAAAAAGCGTCGT CAGCGTCGTCGTGCCAGTGGTCGTTCA		873
	-	*ACCGGTGTCGAC*GGAAGAAGAGACGA CAGG		

❖ Restriction enzyme sites in the primers are underlined

❖ PRK forward primer including TAT HIV domain (33 bp)

Table 3 PCR condition program

		Reverse Transcriptase PCR		
	cDNA	NSP2 (full and deleted) & ORF7	TAT-PKR RBD & Apaf-1 CARD	TAT-PKR RBD-Apaf-1 CARD
1 Cycle	Denaturation	94 °C (5 minutes)	94 °C (5 minutes)	94 °C (5 minutes)
35 Cycles	Denaturation	94 °C (30 seconds)	94 °C (15 seconds)	94 °C (15 seconds)
	Annealing	60 °C (30 seconds)	61 °C (30 seconds)	61 °C (30 seconds)
	Extension	72 °C (1 minute)	68 °C (45 seconds)	68 °C (1 minute)
1 Cycle	Extension	72 °C (10 minutes)	68 °C (10 minutes)	68 °C (10 minutes)

Subcloning into pET-His6-TEV-LIC plasmid

The P-A fragments (Figure 4A) were amplified from the pCR2.1-P-A plasmids with the indicated specific primers (Table 2) and RT-PCR conditions (Table 3) and then inserted into the pET-His6-TEV-LIC plasmid using ligation-independent cloning (LIC) (MacroLab, 2014). The pET-His6-TEV-LIC plasmids were linearized by *Ssp*I restriction enzyme (New England Biolabs, USA) digestion, purified and treated with T4 DNA polymerase (Thermo Scientific, USA) in the presence of dGTP (Thermo Scientific, USA). Likewise, the purified P-A PCR product was treated in the presence of dCTP (Thermo Scientific, USA). Then, 2 µl of each respective T4 treatment reaction was a mixed in a total volume of 10 µL and incubated for 10 min at room temperature (RT) to anneal prior to transformation into BL21 (DE3) cells and selection of a single transformant colony for protein expression. Transformants (pET-P-A) (Figure 4B) were screened for the correct

insertion of the coding fragment and for DNA insert in-frame translation of the N-terminal $(His)_6$ tag by PCR and sequencing analyses.

Subclone into the pQE32 plasmid

The P-A fragment was released from pCR2.1-P-A by *Sma*I and *Sal*I restriction enzyme digestion and inserted into the pQE32 plasmid at the restriction sites following the supplier's instructions and was then transformed into M15 (pREP4) cells. Transformants (pQE32-P-A) (Figure 4C) were checked for the correct coding insertion and in-frame translation of the $(His)_6$ tags by using PCR and sequencing analysis.

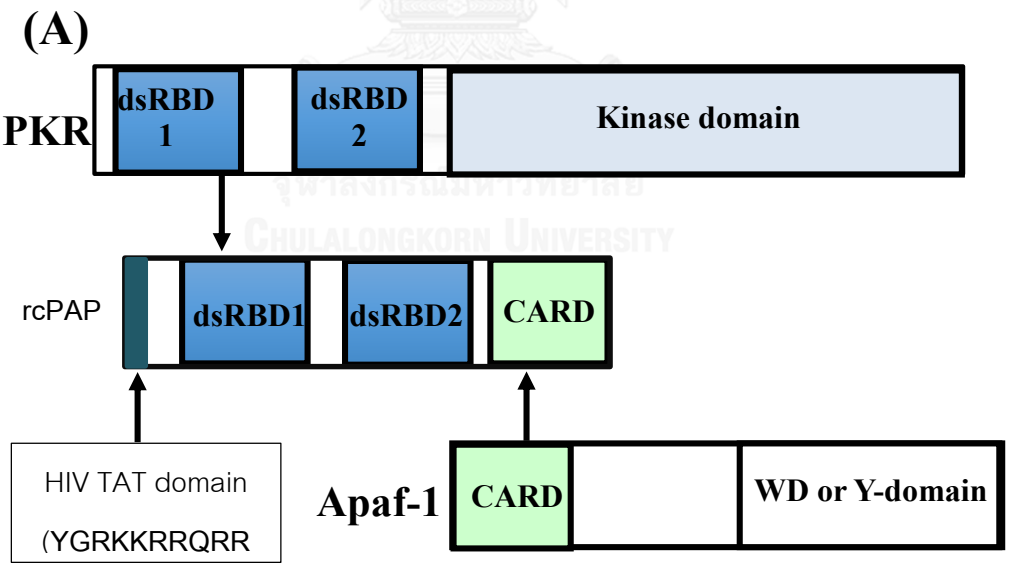

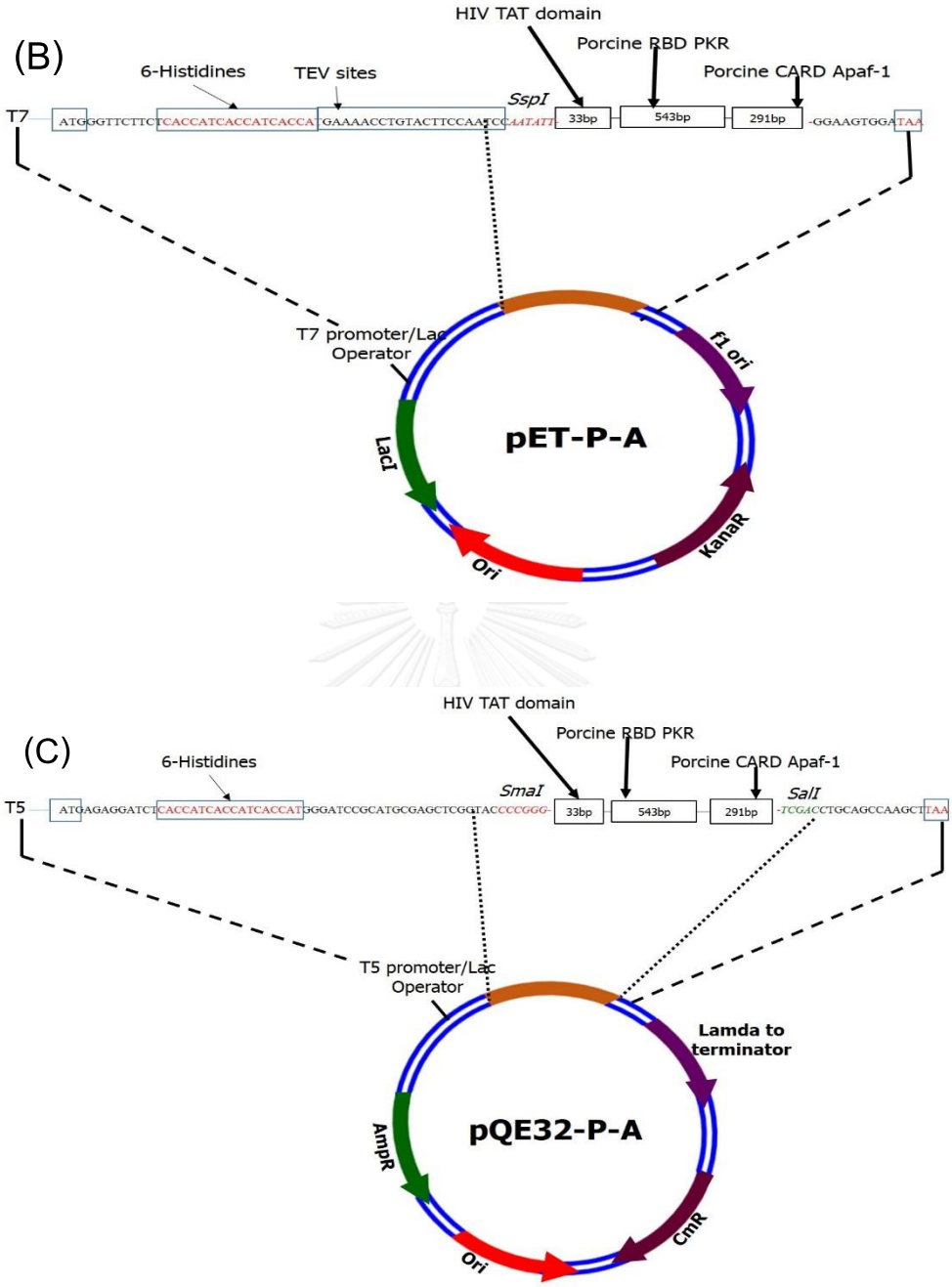

Figure 4. Schematic structure of (A) rcPAP, dsRBD 1 and 2 of swine PKR reconnected to the CARD domain of swine Apaf-1 as indicated; $(His)_6$-tagged rcPAP in the (B) pET-His6-TEV-LIC and (C) pQE32 plasmids.

Expression of rcPAP and optimization of the expression conditions

A single colony of each respective transformant (one for each recombinant plasmid) was propagated overnight in 3 ml of LB media containing the appropriate antibiotic in the correct amount at 37 °C under shaking condition. Then, 500 µl of the overnight culture was inoculated into 10 ml of pre-warmed medium (including antibiotics) and grown at 37 °C with vigorous shaking until the optical density at 600 nm (OD_{600}) of the cell suspension was approximately 0.6. The cultures were divided into two 5-ml fractions, one of which was induced for rcPAP expression by the addition of IPTG to a final concentration of 1 mM, and then cultured for 5 h at the selected temperature (18, 25, 30 and 37 °C). The cells were harvested by centrifugation for 1 min at 12,000 rpm, discarding the supernatant and re-suspending the cell pellet in SDS-PAGE loading buffer (0.2 ml/ml original culture volume), and heated at 95 °C for 5 min before 10 µl was resolved through a SDS-PAGE gel (12.5 % (w/v) acrylamide resolving gel) at 10 V/cm and then stained with Coomassie brilliant blue-R250 (CBB; Bio Basic, Canada). The expression level of the rcPAP from the pET-His6-TEV-LIC and pQE32 plasmids was determined in the stained gels using the ImageJ image analysis software (http://imagej.nih.gov/ij) (Nguyen et al., 2014).

To optimize the expression conditions, the (i) inoculum cell density (as OD_{600} value), (ii) the final IPTG concentration and (iii) the induction time were evaluated in turn by sequential univariate analysis at the optimized temperature (see above). In short, when

the inoculum reached the selected OD_{600} value (0.5, 0.6, 0.7, 0.8, 1 and 1.2), the culture was induced with 1.0 mM IPTG for 5 h, and the yield of rcPAP was evaluated (as above), selecting the OD_{600} value that generates the highest yield. Then, at the optimized temperature and inoculum OD_{600}, the cultures were induced with different final concentrations of IPTG (0, 0.1, 0.25, 0.5, 0.75, 1.0 and 2 mM) for 5 h prior to evaluating the yield of rcPAP, and IPTG concentration that resulted in the highest yield was selected. Finally, using the above selected conditions, the subculture was induced for various times (0, 2, 4, 6, 8, 10, 12 and 18 h) and then the condition generating the highest rcPAP yield was selected.

The three-dimensional (3D) structure of rcPAP

The 3D structure of the rcPAP was predicted from its amino acid sequences using I-TASSER software (http://zhanglab.ccmb.med.umich.edu/I-TASSER/) (Roy et al., 2010).

Solubility of the rcPAP produced within *E. coli*

To test the solubility of the rcPAP produced at various induction temperatures (at otherwise the optimal inoculum OD_{600}, IPTG concentration and induction time), *E. coli* pellets were obtained from 300-ml cell cultures induced with IPTG, re-suspended in lysis buffer (25 mM Tris-HCL, pH 7.4 containing 5 mM MgCl2, 1 % (v/v) Triton-X-100, 1 % (v/v) N-lauroyl-sarcosine and 10 mM imidazole), and then sonicated on ice for 10 min (Vo and Nuntaprasert, 2015). After sonication, the cell suspensions were centrifuged at 12,000

rpm for 10 min at 4 °C. The clear supernatant and pellet were collected and analysed for the rcPAP yield after SDS-PAGE resolution and CBB staining, as above. The solubility level was derived from the percentage of rcPAP in the soluble and pellet fractions at each induction temperature.

Purification of rcPAP

To enrich the rcPAP to apparent homogeneity, the transformed and induced M15 (pQE32-P-A) and BL21 (DE3) (pET-P-A) cell pellets were re-suspended in lysis buffer (as above) and incubated on ice for 1 h. The suspension was then sonicated on ice and centrifuged at 12,000 rpm at 4 °C for 30 min. The levels of rcPAP in the resulting soluble and insoluble fractions were determined after SDS-PAGE resolution and CBB staining, as above. HiTrap chelating affinity column (HiTrap™ Chelating HP, Germany) chromatography was used to enrich the rcPAP. The column was washed with distilled water and recharged with 0.1 M $NiSO_4$ prior to equilibrating with loading buffer. The solubilized lysate was loaded onto the column and washed with the same buffer to remove contaminating *E. coli* proteins. Finally, the rcPAP was eluted with elution buffer containing various concentrations of imidazole (0.1, 0.2, 0.3, 0.4, 0.5 and 1 M). Each purification step was analysed by resolution through SDS-PAGE (12.5 % (w/v) acrylamide resolving gel) with CBB staining and confirmed by western blot analysis. The eluted protein was dialysed against phosphate buffer saline (PBS) overnight using Cellu-Sep® T2 Tubings dialysis

membrane (Seguin, USA). After measuring the protein concentration by the standard bicinchonic acid (BCA) assay (Pierce, USA), the protein solution was aliquoted and stored at -80 °C until further use.

Concentration of rcPAP

The enriched rcPAP concentration was determined as the total protein using a BCA protein assay kit (Pierce, USA) with bovine serum albumin (BSA) at 25–2,000 µg/ml as the reference standard. Briefly, both BSA standards and the unknown protein samples were mixed with the working reagent and incubated at 37 °C for 30 min. The spectrophotometer (GENESYS™ 20 Visible Spectrophotometer, Thermo Scientific, USA) was set at 562 nm and PBS was used as the blank. The protein concentration of each unknown sample was estimated based on the standard curve of the BSA concentration.

Production of polyclonal antibodies against rcPAP in BALB/c mice

The five ml of the purified rcPAP (500 µg/ml) were submitted and the mouse polyclonal antibody against rcPAP was produced by ABGENEX Co. LTD (India).

The immune-reactivity between the enriched rcPAP and the mouse polyclonal antibodies was confirmed using western blot, ELISA and immunofluorescence (IFA) assays.

Western blot analysis

The SDS-PAGE and western blot analyses were performed as described previously (Kim et al., 2013). Briefly, the lysate from the optimally induced bacterial cells expressing rcPAP from the pQE32-P-A and pET-P-A plasmids was separated by SDS-PAGE (12.5 % (w/v) resolving gel) and then transferred to a polyvinyl difluoride membrane (PVDF) (Pall Corporation, USA) in transfer buffer (20 mM Tris-HCl, 192 mM glycine, 0.1 % (w/v) SDS, 20 % (v/v) methanol, pH 8.3) using a semi-dry transfer unit at 25 volts (Amersham, USA) for 1.5 h. The membrane was blocked with 5 % (w/v) skim milk in PBS at 4 °C overnight, washed with PBS/0.5 % (v/v) Tween 20 (PBS-T) and then incubated with a 1: 1,000 dilution of mouse anti-His monoclonal antibodies (GenScript, USA) or a 1: 1,000 dilution of mouse anti-rcPAP polyclonal antibodies at 37 °C for 1 h, washed five times in PBS-T, and then incubated with a 1: 2,000 dilution of horseradish peroxidase (HRP)-conjugated goat anti-mouse IgG (Sigma, USA) at 37 °C for 1 h. After washing (as above), the colour was developed by incubation with 3, 3-diaminobenzidine (Dojindo, Japan) for 15–30 min, and the colour development was terminated by rinsing with distilled water.

Indirect immunofluorescence assay (IFA)

The MARC-145 cells in 24-well plates were incubated with or without 60 μg/ml of rcPAP (Guo et al., 2015) at 37 °C in a 5 % (v/v) CO_2 incubator for 3 h, washed with PBS to remove the medium and then fixed in 4 % (w/v) paraformaldehyde for 10 min at RT. After

washing in PBS, the cells were incubated in 0.1 % (v/v) Triton-X in PBS for 5 min at RT, washed in PBS and then incubated with the mouse anti-rcPAP polyclonal antibodies (1: 500 dilution) overnight at 4 °C. The cells were rinsed five times with PBS and incubated with the Cy2-conjugated AffiniPure goat anti-mouse IgG (Jackson ImmunoResearch, USA) (1: 200 dilution) at RT for 1 h. Finally, the cells were washed five times with PBS, and tetramethylrhodamine isothiocyanate (Thermo Scientific, USA) was added prior to examination using a fluorescence microscope (LSM510 META; Carl Zeiss, Jena, Germany).

Murine anti-rcPAP polyclonal antibody determination by indirect ELISA

Titration of the mouse antiserum against rcPAP was assayed using an indirect ELISA. Briefly, the wells of the ELISA plate were coated with varying concentrations of the purified rcPAP (range 1.56–100 μg/ml/well) in a coating buffer (15 mM Na_2CO_3, 35 mM $NaHCO_3$, pH 9.6) overnight at 4 °C. The wells were washed five times with PBS-T, blocked with 5% (w/v) skim milk in PBS at 37 °C for 1 h, washed five times with the PBS-T and then incubated with 100 μL of antiserum (1: 10 and 1: 50 dilutions) at 37 °C for 1 h. After incubation, the wells were washed five times with PBS-T and then incubated with 100 μL of the 1: 10,000 dilution of HRP-conjugated goat anti-mouse IgG (Sigma, USA) at 37 °C for 1 h. Following five washes with PBS-T, the wells were reacted with 3, 3′, 5, 5′-tetramemethylbenzidine at RT in a dark room for 15 min, and then the reaction was

stopped by the addition of 100 µL of 2 M H_2SO_4. The absorbance was measured at 450 nm using an ELISA plate reader (Multiskan EX, Thermo Scientific, USA).

Results

Construction and expression of rcPAP

The rcPAP plasmids were successfully constructed and produced from the US strain of PRRS virus-infected PAM (Vo and Nuntaprasert, 2015). The nucleotide and deduced amino acid sequences of the dsRBD of the swine PKR gene and the CARD domain of the swine CARD Apaf-1 gene were analysed (data not shown), and the sequences were submitted to GenBank (accession numbers KP729189 and KP729186, respectively).

The P-A cDNA was successfully constructed into the pET-His6-TEV-LIC and pQE32 plasmids, respectively. The sequences of each plasmid confirmed their correct orientations and in-frame positions with the N-terminal $(His)_6$ tag (data not shown). After transformation into the respective host *E. coli* strain, small-scale expression of rcPAP was induced by the addition of 1 mM IPTG. The rcPAP was successfully expressed from both expression plasmids using the respective *E. coli* systems (Figure 5). The molecular weight of rcPAP was determined to be approximately 35 kDa from the deduced amino acid sequence, which was in agreement with the observed protein band on the SDS-PAGE analysis of the rcPAP expressed in both the pET-His6-TEV-LIC and pQE32 plasmids (Figure 5), with a single band at an apparent molecular mass of 35 kDa.

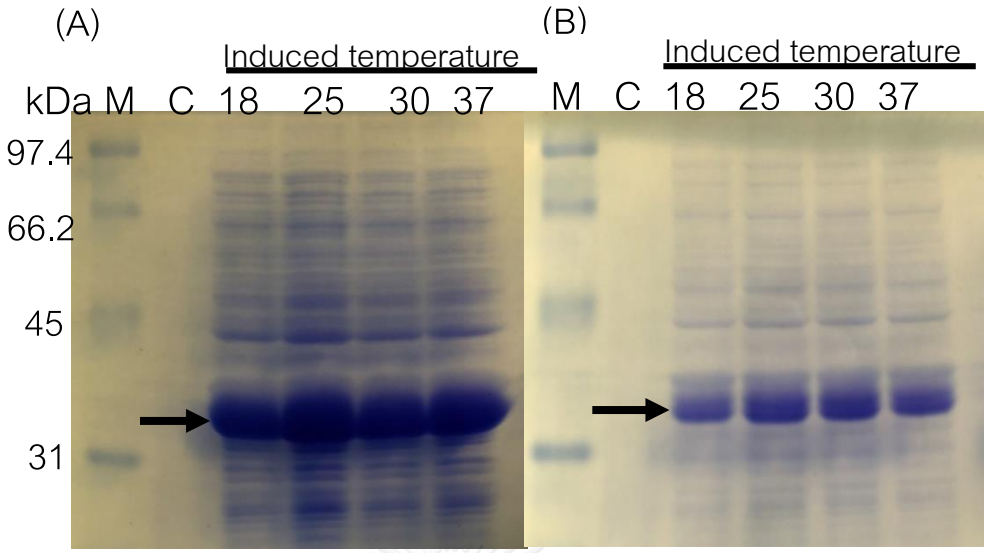

Figure 5. Analysis of the rcPAP produced from the (A) pET-His6-TEV-LIC and (B) pQE32 plasmids at varying induction temperatures. The rcPAP was resolved through 12.5 % (w/v) acrylamide SDS-PAGE and stained with CBB. M, protein markers (kDa); C, total cell protein before IPTG induction as a negative control. The protein markers (BioRad) on the gels are indicated in kilodaltons (kDa).

The expression levels of recombinant proteins in *E. coli* typically vary according to the plasmid and temperature (Rosano and Ceccarelli, 2014). In this study, the expression levels of rcPAP produced from the pET-His6-TEV-LIC plasmid at 37 °C in BL21 (DE3) cells (19.5 %) were 2.4-fold higher than that obtained from the pQE32 plasmid in M15 (pREP4) cells (8.1 %) under the same conditions (Table 4). However, at a lower temperature (25 °C) the rcPAP expression levels increased just over 1.1-fold to 22.7 % and 9.1 % for the pET-His6-TEV-LIC and pQE32 plasmids, respectively (Table 4). The rcPAP produced from both expression plasmids successfully reacted with the mouse anti-His monoclonal antibodies, as determined by western blot analysis (Figure 6). The rcPAP

produced from the pET-His6-TEV-LIC plasmid showed a stronger band on the membrane than that of the pQE32 plasmid, consistent with its 2.4-fold higher expression level (see above). Because rcPAP was produced at a higher level from the pET-His6-TEV-LIC plasmid (in BL21 (DE3) cells), this expression system was selected for further study.

Table 4 Expression levels of rcPAP at the different-induction temperatures

Plasmids	Expression level (%)			
	18 °C	25 °C	30 °C	37 °C
pET-His6-TEV-LIC	9.3	22.7	16.7	19.5
pQE32	6.4	9.1	8.2	8.1

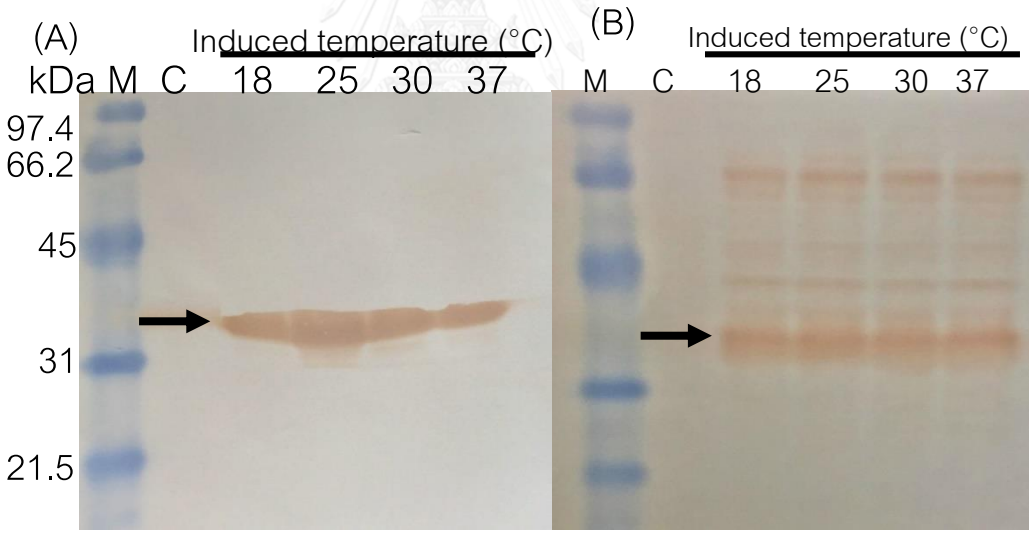

Figure 6. Western blot analysis of the rcPAP using mouse anti-His_6 monoclonal antibodies from the (A) pET-His6-TEV-LIC and (B) pQE32 plasmids. M, protein markers (kDa); C, total cell protein before IPTG induction as a negative control. The protein markers (BioRad) on the gels are indicated in kDa.

Determining the 3D-structure of a novel protein is the cornerstone of many aspects of modern biology (Roy et al., 2010). In this study, the 3D structure of rcPAP was evaluated theoretically using I-TASSER (Figure 7 and Table 5). Five models of rcPAP were computationally generated using the I-TASSER algorithm with C-scores ranging from -4.27 to -4.52, where the C-score is a confidence score and ranges from -5 to 2, with higher scores representing a higher confidence level in the model (Roy et al., 2010). Model 1, with a C-score of -4.27, was used for all of the analyses described (Figure 7A). The overall structure of the rcPAP contained 13 α-helices and seven β-strands (α-α-α-β-β-β-α-α-β-β-β-α-α-α-α-α-α-α-α). In addition, the 3D structure of the dsRBD of porcine PKR protein was predicted (C-score of 0.69) to contain four α-helices and six β-strands (α-β-β-β-α-α-β-β-β-α), while the CARD domain of the porcine Apaf-1 protein was predicted (C-score of 0.93) to contain six α-helices. These results indicated that the 3D structure of rcPAP had three more α-helices (one each from the plasmid, the TAT domain of HIV and the linker between the dsRBD and CARD domain) and one more β-strand than the sum of the dsRBD of the porcine PKR and the CARD domain of the porcine Apaf-1 proteins. The TM-score ranged from 0 to 1, and the closest structural similarity was used to predict the I-TASSER model (Roy et al., 2010). In this study, the closest structural matches of the dsRBD of swine PKR protein (TM-score = 0.82) and the CARD domain of swine Apaf-1 (TM-score = 0.975) protein were similar to the human PKR (1QU6A) and human Apaf-1 (1Z6TB) proteins, respectively. Due to having highest level of structural

similarity (TM-score = 1), these proteins may well have a similar function as the target (Asano et al., 2004; Roy et al., 2010).

Table 5 The 3D structural prediction of rcPAP based on the deduced amino acid sequences using the I-TASSER method

Items	α-helices	β-strands	C-score
rcPAP model 1	13	7	-4.27
rcPAP model 2	13	7	-4.5
rcPAP model 3	13	7	-4.35
rcPAP model 4	13	7	-4.45
rcPAP model 5	13	7	-4.52
dsRBD of porcine PKR protein	4	6	0.69
CARD domain of porcine Apaf-1 protein	6	0	0.93

(A)

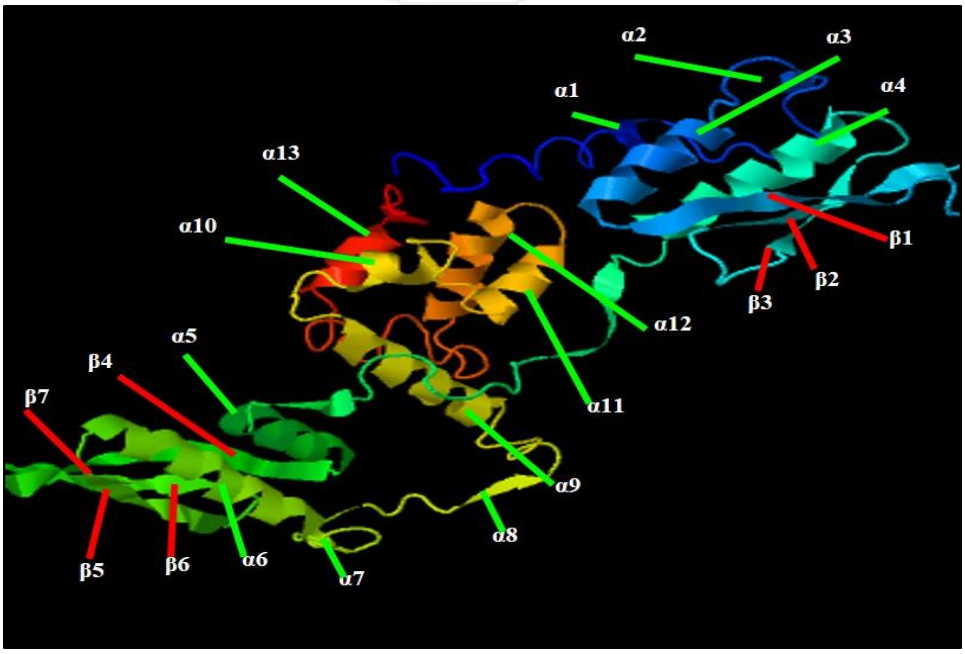

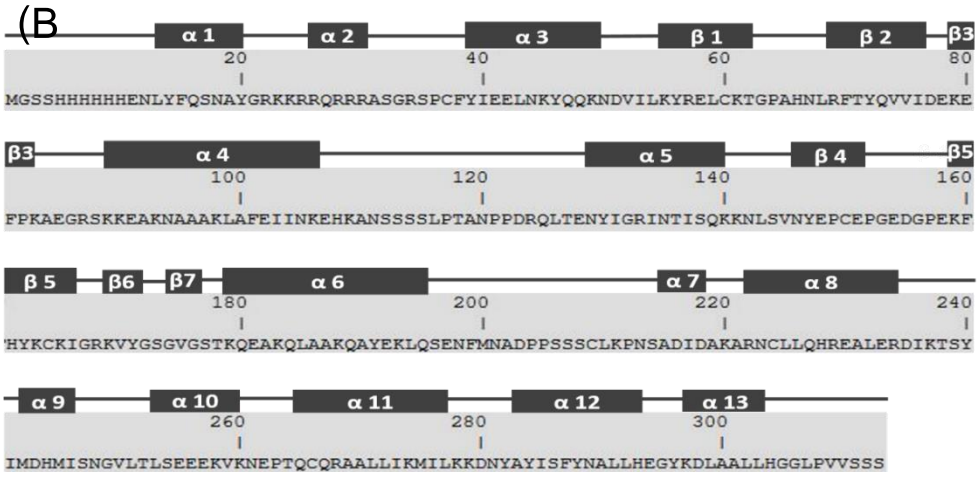

Figure 7. (A) Ribbon depiction of the I-TASSER model of rcPAP (http://zhanglab.ccmb.med.umich.edu/I-TASSER/) and (B) the secondary structure topology of rcPAP (http://zhanglab.ccmb.med.umich.edu/I-TASSER/).

Solubility test of rcPAP

The proportion and yield of soluble recombinant proteins produced often depend on the induction temperature (Francis and Page, 2010), and the protein expression at low temperature often significantly improves the solubility of recombinant proteins (Francis and Page, 2010). Accordingly, the lower level of protein solubility was found at higher temperatures (8.98 % and 3.1 % at 30 °C and 37 °C, respectively) than at lower temperatures (11.7 % and 19.8 % at 18 °C and 25 °C, respectively) (Figure 8 and Table 6).

Table 6 Solubility of rcPAP produced from the pET-His6-TEV-LIC plasmid at different induction temperatures

Items	Solubility level (%)			
	18 °C	25 °C	30 °C	37 °C
Soluble fraction	11.7	19.8	8.98	3.1
Pellet	9.02	17.2	15.5	14.7

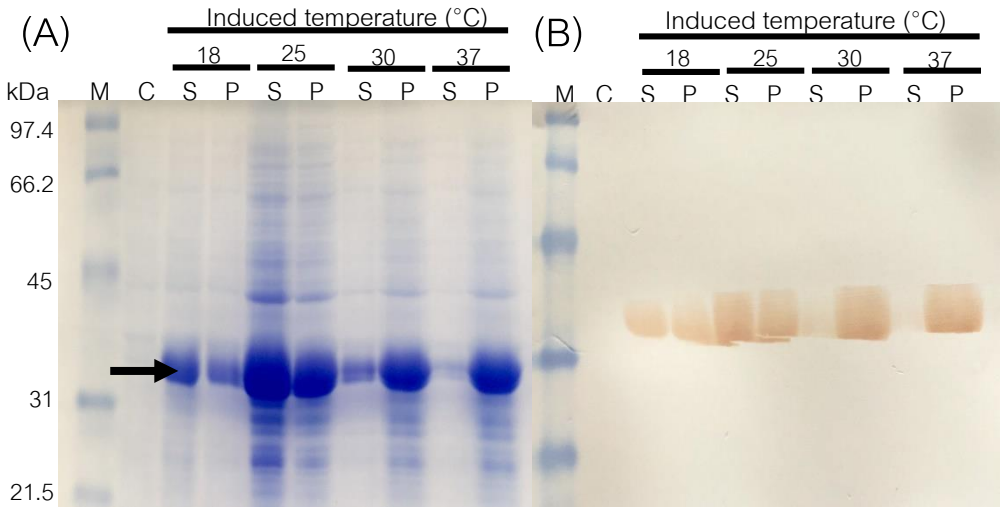

Figure 8. Solubility level of rcPAP produced from the pET-His6-TEV-LIC plasmid /BL21(DE3) cells at varying-induction temperatures, showing the (A) 12.5 % (w/v) acrylamide SDS-PAGE gel after CBB staining and (B) the western blot analysis with mouse anti-His monoclonal antibodies. M, protein markers (kDa); C, total cell protein before IPTG induction as a negative control; P, pellet fraction after cell sonication; S, soluble supernatant after cell sonication. The protein markers (BioRad) on the gels are indicated in kDa.

Optimization of rcPAP expression

The optimal expression conditions for rcPAP production from the pET-His6-TEV-LIC plasmid were evaluated sequentially in terms of the inoculum cell density (as OD_{600} value), the IPTG concentration and the induction time at 25 °C (the previously determined optimal temperature) in a univariate approach that assumes no significant interaction between these three factors. Within that caveat, the optimal OD_{600} was found to be 0.6 (Figure 9A), the optimal IPTG concentration was 0.75 mM (Figure 9B), and the induction

time was 18 h (Figure 9C), yielding the optimal induction conditions of an inoculum OD_{600} of 0.6, induced with 0.75 mM IPTG for 18 h at 25 °C.

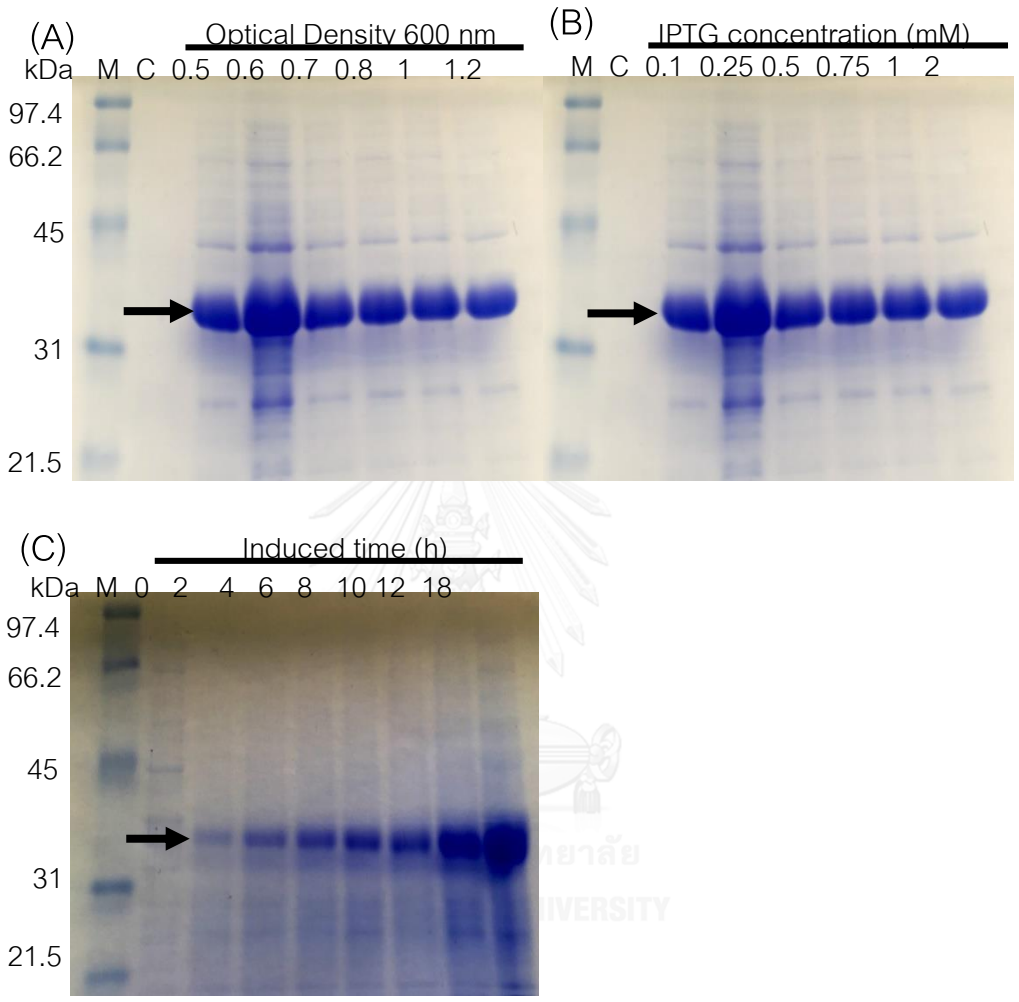

Figure 9. Optimization of the (A) the inoculum cell density (as OD_{600} values), (B) the IPTG concentration and (C) the induction time for rcPAP production at 25 °C, as determined after resolution in 12.5 % (w/v) acrylamide SDS-PAGE and CBB staining. (A) *E. coli* transformants were inoculated at different densities and incubated with 1 mM IPTG and induced for 5 h. (B) *E. coli* transformants were inoculated at OD_{600} of 0.6 and induced for 5 h. (C) *E. coli* transformants were inoculated at OD_{600} of 0.6 and induced with 0.75 mM IPTG. M, protein markers (kDa); C, total cell protein before IPTG induction as a negative control. The protein markers (BioRad) on the gels are indicated in kDa.

Purification of rcPAP

The rcPAP purification was designed to remove most contaminating *E. coli* proteins to give an acceptable level of rcPAP purity. The rcPAP was produced from the pET-His6-TEV-LIC plasmid under the optimal induction conditions (see above), where rcPAP was mainly found in the soluble fraction, and therefore, its purification could be performed under a native condition from the HiTrap chelating affinity column. After extensive washing, the bound rcPAP was eluted with various concentrations of imidazole ranging from 100 mM to 1 M. The bound rcPAP started to elute at 200 mM of imidazole and reached the highest yield at 0.5 and 1 M of imidazole (Figure 10). The SDS-PAGE and the western blot analysis of the eluates showed a single band with a molecular mass of approximately 35 kDa (Figure 10), and therefore, the rcPAP was enriched to apparent homogeneity. In addition, rcPAP was found in varying fractions eluted with 0.5 M of imidazole (Figure 11 and Table 7). The rcPAP concentration of fraction 3 (14.21 mg/l of bacterial culture) showed the highest yield followed by fraction 2 (4.73 mg/l of bacterial culture). Moreover, after dialysis against PBS, the recovery yield of rcPAP was 12.32 mg/l of bacterial culture. In this study, 55.2 % (12.32/22.31) of the rcPAP was recovered from 84.8 % (22.31/26.31) of the eluted protein.

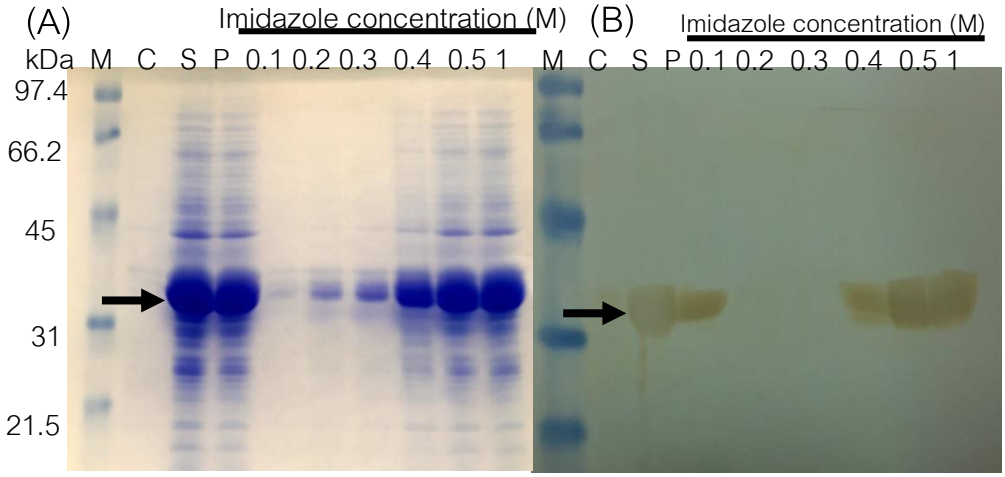

Figure 10. Enrichment of rcPAP using a HiTrap chelating HP column. (A) The 12.5 % SDS-PAGE gel stained with CBB and (B) the western blot analysis of rcPAP using mouse anti-His monoclonal antibodies. M, protein markers kDa; C, total cell protein before IPTG induction as a negative control; S, soluble supernatant after cell sonication; P, pellet fraction after cell sonication; Lanes 0.1–0.5 and 1, eluted with 100, 200, 300, 400, 500 and 1000 mM imidazole, respectively. The protein markers (BioRad) on the gels are indicated in kDa.

Table 7 Concentrations (mg/L) of the rcPAP fractions

Fractions	Yields of rcPAP (mg/l)
Soluble	26.31
Flow through	0.07
Elution 1	1.63
Elution 2	4.73
Elution 3	14.21
Elution 4	1.13
Elution 5	0.61
Dialyzed rcPAP	12.32

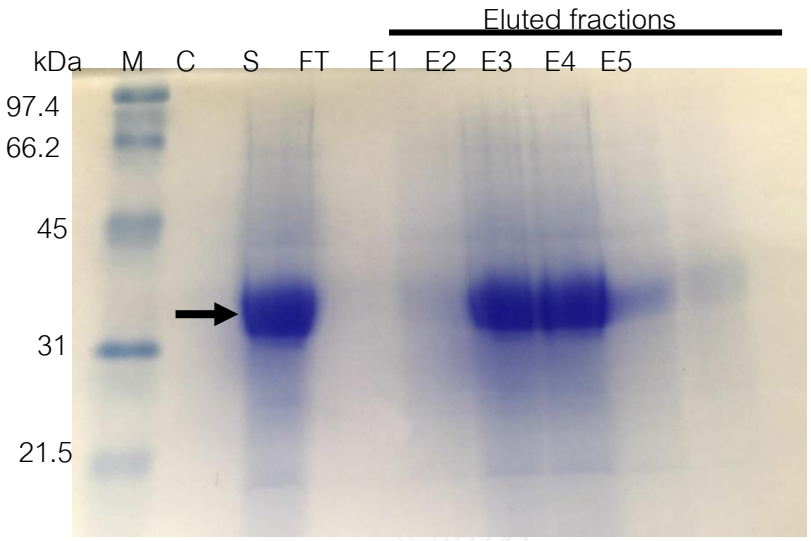

Figure 11. Enrichment of rcPAP via HiTrap chelating HP column chromatography. The rcPAP was resolved by 12.5 % (w/v) acrylamide SDS-PAGE gel and stained with CBB: M, protein markers kDa; C, total cell protein before IPTG induction as a negative control; FT, flow through; E1–5, fractions 1 to 5, respectively, with 0.5 M of imidazole. The protein markers (BioRad) on the gels are indicated in kDa.

Characterization of mouse polyclonal antibody against rcPAP

The western blot analysis revealed that the purified rcPAP reacted with the mouse polyclonal antibody to reveal a single band of 35 kDa (Figure 12). The purified rcPAP was coated on ELISA plates at different concentrations (1.56 to 100 µg/ml/well). The mouse polyclonal antibodies raised against rcPAP exhibited concentration-dependent binding to rcPAP and the antisera at a 1: 10 dilution showed a 1.15-fold higher binding value in ELISA than the 1: 50 dilution (Figure 13A). The apparent specificity of the mouse polyclonal antibodies against rcPAP was also shown in the IFA test (Figure 13B), as no reaction was observed in untransformed cells in contrast to the transformed and induced cells that

expressed rcPAP. The rcPAP was located in the cytoplasm (red colour) of the MARC-145 cells (Figure 13B-C1). The rcPAP expressed in *E. coli* was able to elicit an rcPAP-specific antibody response.

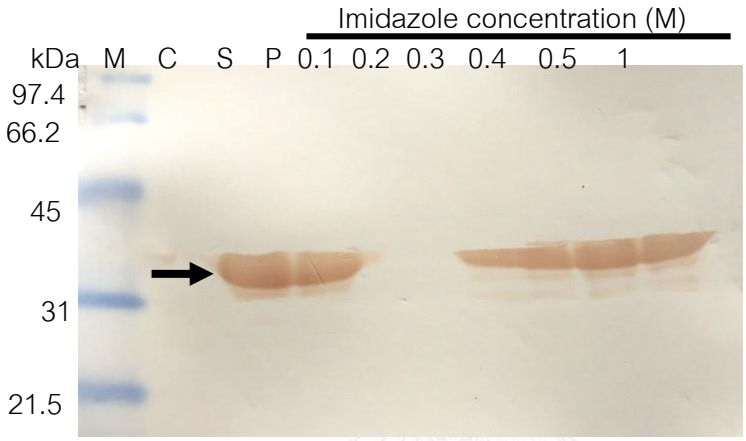

Figure 12. Western blot analysis of rcPAP using mouse anti-rcPAP polyclonal antibodies. M, protein markers kDa; C, total cell protein before IPTG induction as a negative control; S, soluble supernatant after cell sonication; P, pellet fraction after cell sonication; lane 0.1, eluted with 100 mM imidazole; Lanes 0.1–0.5 and 1, eluted with 100, 200, 300, 400, 500 and 1000 mM imidazole, respectively. The protein markers (BioRad) on the gels are indicated in kDa.

(A)

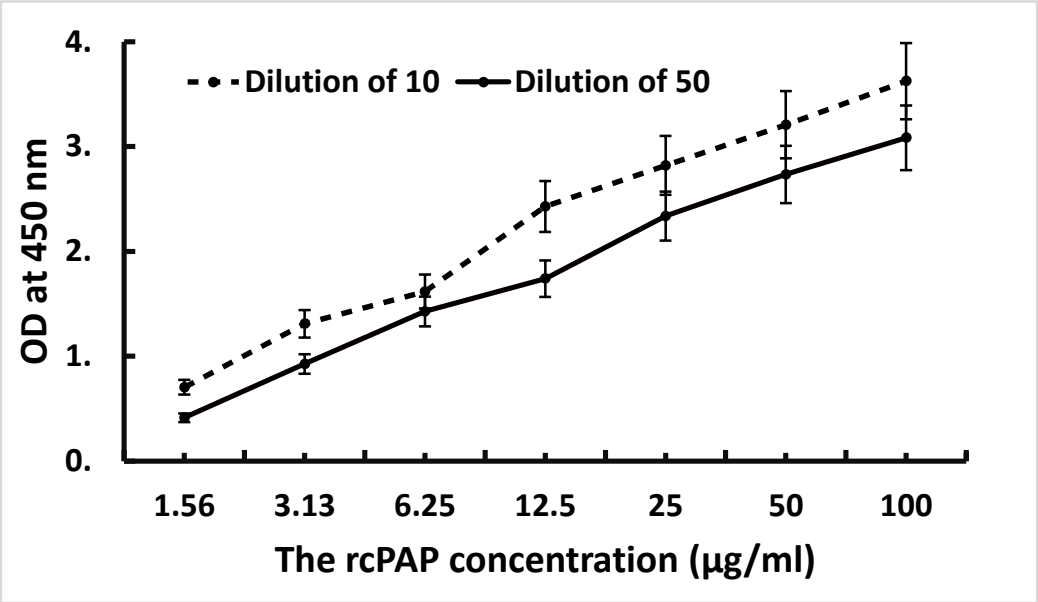
4.
3.
2.
1.
0.
OD at 450 nm
Dilution of 10
Dilution of 50
1.56
3.13
6.25
12.5
25
50
100
The rcPAP concentration (µg/ml)

(B)

C1

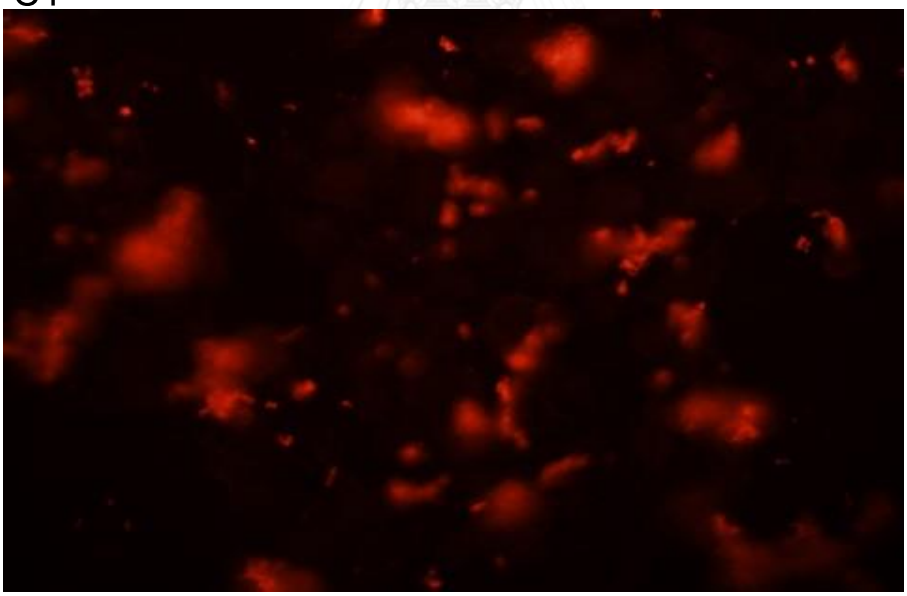

C2

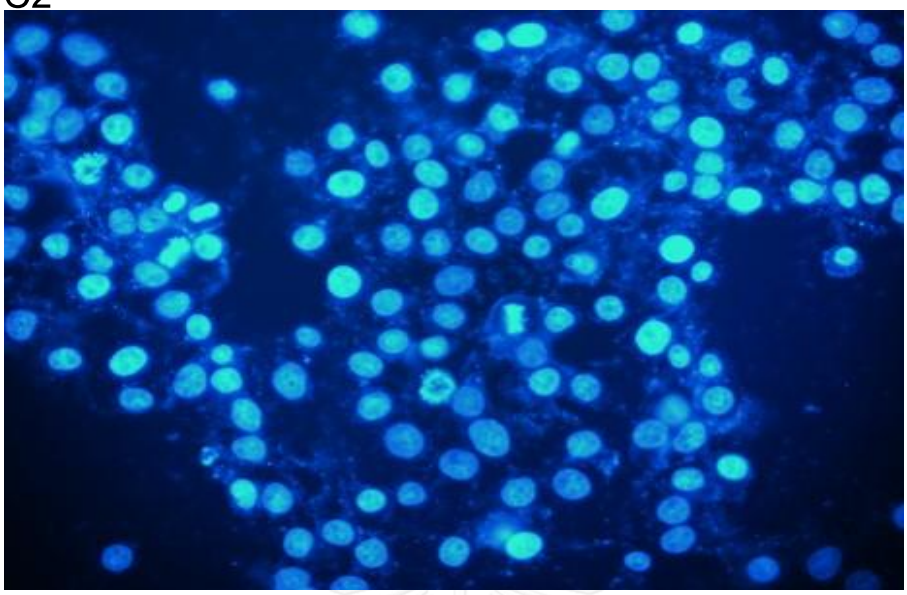

C3

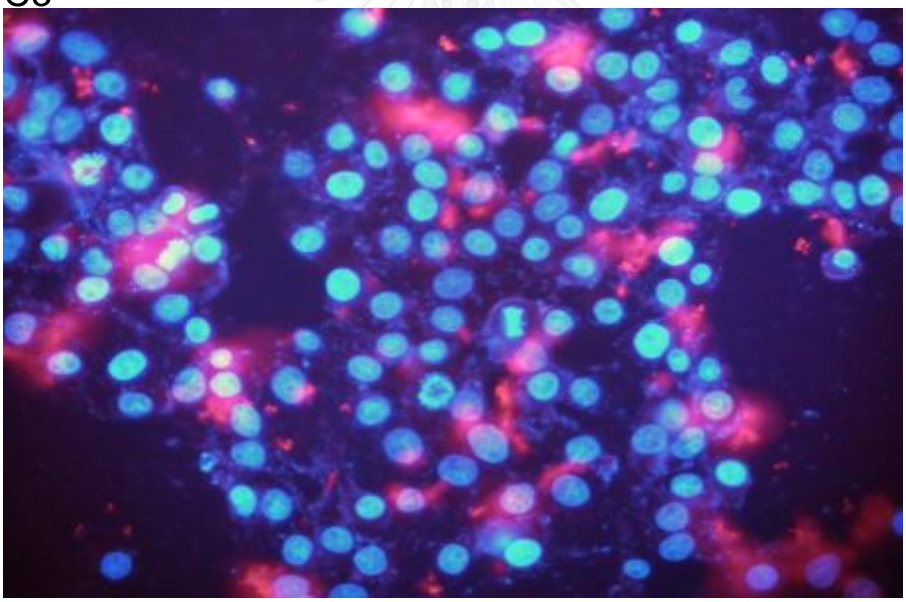

Figure 13. Characterization of mouse anti-rcPAP polyclonal antibodies by (A) indirect ELISA and (B) IFA analysis on MARC-145 cells. (A) The OD450 values represent the average of five independent experiments performed in six replicates. Error bars indicate the standard deviations. (B) C1, the rcPAP are displayed in red; C2, the cell nuclei are shown in blue; C3, merged.

Discussion

In general, there are several mechanisms that the body can use to reduce and/or to cope with infections. The use of a recombinant chimaeric protein, such as that used in this study, is an example of limiting or reducing the viability and number of virus-infected cells during an infection to potentially reduce the viral load. The induction of apoptosis (cell death) may benefit limiting the virulence of intracellular viruses by shortening their survival, especially for some important PRRS virus in pigs that have evolved mechanisms to inhibit apoptosis. The expression and production of recombinant proteins from the full-length PKR and Apaf-1 genes in humans and mice have been reported (Meurs et al., 1990; Rende-Fournier et al., 1997; Zhou et al., 1999; Riedl et al., 2005; Reubold et al., 2011). Many reasons, including their ease of generation, have increased their successful clinical use and non-toxic nature upon injection to animals, thus justifying the use of targeting chimaeric peptides instead of entire proteins for the production of those genes. As an un-natural anti-viral mechanism, this rcPAP with its three different parts (TAT domain from HIV, dsRBD of the swine PKR and the CARD domain of swine Apaf-1), was successfully constructed from PAM infected with the Thai-isolated US strain PRRS virus and produced in a bacterial expression system.

Two bacterial expression plasmids (pET-His6-TEV-LIC and the pQE32) were used to express the N-terminus $(His)_6$ tagged rcPAP chimaera, and the expression levels of the

resulting fusion protein at different induction temperatures were evaluated. The rcPAP expression levels depended on the induction temperature and the expression plasmid/host cell system, but the N-terminus $(His)_6$ tag did not interfere with the expression levels of the chimaeric protein. The pET-His6-TEV-LIC plasmid in the BL21 (DE3) cells showed a higher rcPAP expression levels at all induction temperatures than the pQE32 plasmid in the M15 (pREP4) cells, which may reflect differences in the replicon, promoter and host cell between the two expression systems. This is in agreement with previous reports that pET plasmids with the pMB1 origin (ColE1-derivative) have a higher copy number per cell than those with the wild-type ColE1 origin in the pQE plasmids (15–60 vs. 15–20 copies per cell, respectively) (Rosano and Ceccarelli, 2014).

The higher plasmid dosage may well result in a higher recombinant protein yield (Boustanshenas et al., 2013). Indeed, the yield of recombinant proteins produced from the pET plasmids were reported to be two-fold higher than those from the pQE plasmid (QIAGEN, USA) (Suryanarayana et al., 2016), in agreement with the results of this study. Moreover, the yield of soluble protein can be increased by varying the induction temperature, the inducer concentration and the inoculum OD_{600} (Gupta and Shukla, 2015). In particular, protein expression at a low temperatures often results in a significantly improved solubility of the recombinant protein (Gupta and Shukla, 2015). Accordingly, the rcPAP produced from the pET-His6-TEV-LIC plasmid at induction at lower temperatures (18–25 °C) yielded a higher amount of soluble rcPAP (without modifying the native protein

extraction method), indicating that a slow induction of the rcPAP efficiently reduced the formation of inclusion bodies (Rosano and Ceccarelli, 2014).

The computational modelling of the protein 3D structure of rcPAP was performed using I-TASSER (Iterative Threading Assembly Refinement) along with those for the dsRBD of the swine PKR protein and the CARD domain of the swine Apaf-1 protein (Roy et al., 2010). The C-scores of the obtained rcPAP structures ranged from -4.27 to -4.52. Although -1.5 has been used previously as a cutoff for confidence in models, there can still be significant modelling accuracy in models with C-scores below this limit (Roy et al., 2010). Considering the similarities in structural features, the TM-score of the dsRBD of the swine PKR protein and the CARD domain of the swine Apaf-1 protein that matched the best I-TASSER model was aligned in the PDB library, the results of which suggested that the dsRBD of the swine PKR protein and the CARD domain of the swine Apaf-1 protein will be likely to have the same function as the human PKR and Apaf-1 proteins, respectively.

Due to the relatively high expression yield and solubility of the rcPAP obtained at 25 °C, the effect of the inoculum cell density, the IPTG concentration and the induction time were optimized to improve the protein expression yield. Generally, low-temperature induction in *E. coli* results in the expression of soluble foreign proteins, but high concentrations of IPTG show increased toxicity in *E. coli* and inhibit cell growth (Onodera et al., 1996; Sørensen and Mortensen, 2005; de Groot and Ventura, 2006). Here, it was

found that increasing the inoculum cell density up to an OD_{600} of 0.6 increased the subsequent yield of rcPAP, but at OD_{600} values above 0.6, there was no significant increase in rcPAP yield. Likewise, a prolonged induction time of more than 18 h (data not shown) or an IPTG concentration above 0.75 mM did not significantly enhance the rcPAP expression yield. Thus, the optimized expression conditions for rcPAP were to use an inoculum cell density of an OD_{600} of 0.6 and to induce protein expression by 0.75 mM IPTG at 25 °C for 18 h.

The enrichment of the soluble rcPAP without recovery of the insoluble protein saved time and cost, primarily due to the removal of the cross-flow filtration, denaturing and refolding steps (Kim et al., 2013). The rcPAP were expressed in a soluble form at a low-induction temperature and enriched under a native condition using a HiTrap chelating HP column charged with Ni^{2+}. Although some (29.6%) of the rcPAP was lost during the enrichment, this was expected, as not all of the protein can be recovered without also picking up contaminants. Future studies could address the use of other suitable column chromatography methods, other types of HiTrap media and/or types of salt and salt concentrations used to dilute rcPAP prior to using a HiTrap Chelating HP column.

We also studied the immunogenicity of rcPAP in BALB/c mice. rcPAP in combination with Freund's adjuvant elicited a humoral response in BALB/c mice. The humoral response was characterized by a high titre of polyclonal antibodies, as revealed by indirect ELISA. Furthermore, the anti-rcPAP polyclonal antibodies raised in the BALB/c mice appeared to be specific for rcPAP relative to *E. coli* proteins, as observed by western

blot and IFA analyses. Thus, the rcPAP produced and enriched from *E. coli* might maintain its natural 3D structure, or at least for these immunogenic sites.

Previous studies have shown that the PRRS virus stimulates anti-apoptotic pathways in MARC-145 cells and PAMs in the early infection stage during viral replication, while PRRS virus-infected cells die from apoptosis in the late infection stage after viral replication and assembly and therefore release the new virions (Heijbel, 2003; Costers et al., 2008). If rcPAP could induce apoptosis in MARC-145 cells that were infected with the PRRS virus at an early stage, this would potentially prevent viral replication and assembly and thus reduce the viral load in the swine. In viral-infected cells, when two or more dsRBDs of the rcPAP were cross-linked on the same-viral dsRNA, the effector domain of rcPAP would theoretically then activate caspase 9 and trigger apoptosis (Elmore, 2007; Rider et al., 2011). In this study, the TAT domain of HIV (protein transduction) was used for the delivery of rcPAP into MARC-145 cells. The HIV TAT domain has previously been used to deliver the human DRACO protein into mouse cells and approximately 11 human cell lines (Rider et al., 2011). In swine, the HIV TAT domain has also been shown to deliver the PRRS virus nucleocapsid and the matrix protein into the PK-15 cell line, dendritic cells and peripheral blood mononuclear cells (Jeong et al., 2010). Accordingly, this study demonstrated that rcPAP was transduced_into the cytoplasm of MARC-145 cells, as revealed by the IFA analysis (Figure 11B). Thus, we imply that the HIV TAT domain successfully delivered rcPAP through the MARC-145 cell membrane. For dsRNA detection by rcPAP, the dsRBD of PKR protein was selected to recognize and bind to viral

dsRNA in virus-infected cells (Rider et al., 2011; Guo et al., 2015). Considering the similarities in structural features, it has been suggested that swine PKR protein has a similar function to other mammalian PKR proteins (Asano et al., 2004). This study supported that the dsRBD of the swine PKR gene could recognize viral dsRNA in PRRS virus-infected cells. For the effector domain of rcPAP, the CARD domain from the Apaf-1 gene was chosen for recruitment and activation of the initiator apoptotic pathway (Rider et al., 2011). This study is the first report that utilized the CARD domain of the swine Apaf-1 protein as an apoptosis inducer.

In conclusion, rcPAP was expressed and enriched under native conditions, and its expression could be optimized. This is the first study to produce rcPAP in an *E. coli* expression system. Based on our findings, enriched rcPAP may facilitate further development of more useful methods against PRRS.

CHAPTER 2

The effect of recombinant chimaeric swine PKR-Apaf-1 proteins on PRRS virus-infected MARC-145 cell line

Abstract

We produced the recombinant chimaeric swine PKR-Apaf-1 proteins (rcPAP) from bacteria according to the human DRACO concept. In this study, we explore the possibility that enhanced antiviral activity of this molecule against PRRS in swine. The rcPAP (at a concentration of 40, 60, 80 and 120 μg/ml) was used to treat at 6 h after Thai-isolated US strain PRRS virus-infected MARC-145 cells. The antiviral efficacy with the apoptotic induction to kill virus-infected cells, using MARC-145 cell lines was determined at a time course of 24, 48 and 72 hpi. The results demonstrated that no cell cytotoxicity was observed during rcPAP added and rcPAP was transduced into the MARC-145 cells within 1 h. The induction of cell death and the reduction of PRRS viral replication have responded in a dose dependent manner. The rcPAP concentration of 80 μg/ml at 72 hpi significantly showed the highest enhancement of antiviral activity ($p < 0.05$). The rcPAP significantly increased the monkey active caspase-3 levels at the level of 16.09 fold (13.36 ± 0.003 vs 0.83 ± 0.003 ng/mg protein) in PRRS virus-infected cell lines when treated with 80 μg/ml rcPAP at 72 hpi, ($p < 0.05$). The PRRS viral RNA copy numbers at 72 hpi had significantly reduced by 75.55 % (1.75 ± 0.008 vs 7.16 ± 0.009 log10 (copies/ml)) in the infected cells and 84.47 % (1.02 ± 0.002 vs 6.57 ± 0.02 log10 (copies/ml)) in culture supernatants when treated with 80 μg/ml rcPAP ($p < 0.05$). Interestingly, the viral titers at 72 hpi were dramatically reduced by 87.76 % (0.63 ± 0.004 vs 5.15 ± 0.01 log10 $TCID_{50}$/ml) in PRRS

virus-infected cell lines treated with rcPAP (80 μg/ml) ($p < 0.05$). The results also showed that the rcPAP was able to reduce and suppress N protein synthesis in the PRRS virus-infected cell lines. In conclusion, this study suggested that rcPAP is a promising therapeutic agent against homologous strain PRRS viral infection.

Keywords: Antiviral activity, cell culture, cytotoxicity, in vitro, viral copy number, viral titer, PRRS.

Introduction

The limited number of available antiviral drugs may reflect the difficulties of developing therapeutics to treat viral diseases of both a practical and financial level (Pozzo and Thiry, 2014). Because of being obligate intracellular parasites, the replication of viruses is intricately linked to normal cell processes and thus many compounds such as antiviral drugs that interfere with viral replication are inherently toxic to host cells and present a low therapeutic index (Quinn et al., 2015). Moreover, there is evidence about new variant strains of some swine viruses that are resistant to antiviral drugs and may become more powerful like super-viruses (Rider et al., 2011; Song et al., 2015; Zhou et al., 2015). Therefore, novel antiviral molecules to inhibit PRRS virus replication or enhanced antiviral activity against PRRS virus are welcome options to complement other strategies for PRRS prevention and control.

The ideal antiviral molecules, which are therapeutically safe and effective, would selectively affect specific processes of the target virus with minimal side effects on normal cellular pathways. There are many reports showing the antiviral activity against viral diseases in swine. For example, the RNA interference has been reported as antiviral drugs which target viral genome or viral receptors (Choi et al., 2009; Xiao et al., 2011; Moghaddam et al., 2014; Abba et al., 2015; Li et al., 2015; Liwei et al., 2015). Secondly, plant extract compounds have been studied to inhibit viral replication or viral infection or directly destroy the viral particles (Yang et al., 2013; Moghaddam et al., 2014; Abba et

al., 2015). Thirdly, recombinant proteins have been reported as antivirals which could induce apoptosis and kill viral-infected cells (Rider et al., 2011; Zhang et al., 2013; He et al., 2014; Guo et al., 2015).

One of the options would be to use PRRS virus-specific and efficacious antiviral molecule like rcPAP. The rcPAP has successfully produced from bacterial system (Vo and Nuntaprasert, 2015, 2016) according to human DRACO concept. The rcPAP is consisted of TAT domain of HIV, dsRBD of swine PKR and CARD domain of swine Apaf-1. The rcPAP detects viral dsRNA in viral infected cells via the dsRBD of swine PKR. After two or more rcPAP molecule crosslink on the same viral dsRNA, the rcPAP induces apoptosis and kills those virus-infected cells. An alternative approach to induce apoptosis in infected cells and inhibit viral mRNA expression or translation, the rcPAP molecule produced from bacteria was carried out to study the in vitro effect against PRRS virus.

Materials and Methods

Cell culture, rcPAP and virus

MARC-145 (ATCC: CRL-12231) cell line was cultured in Dulbecco's modified Eagle's medium (DMEM) supplemented with 10% fetal bovine serum (FBS) and maintained at 37 °C in 5 % CO_2 incubator (Ma et al., 2013). The rcPAP (stock at 1 mg/ml) was used at a four concentrations of 40, 60, 80 and 120 μg/ml). US strain PRRS virus (Thai isolated 01NP01, stock virus at 6 log10 $TCID_{50}$/ml) was used in this study. PRRS virus was propagated in MARC-145 cells.

Cytotoxicity assay

The cytotoxicity of rcPAP was evaluated using MTT assay in normal MARC-145 cells in six independent experiments. Each experiment involved triplicate wells per concentration. MACR-145 cells were detached using 0.5 % Trypsin/EDTA (Invitrogen, USA), re-suspended in complete medium and then dispensed into 96-well plates at a density of 10^4 cells per well. After incubation for 24 h, the rcPAP were administered to the wells at varying final concentrations (40, 60, 80, and 120 μg/ml) (Guo et al., 2015) and incubated at 37 °C, in a humidified 5 % CO_2 incubator for 72 h. Then, 10 μl of MTT reagent (5 mg/ml) (Dojindo, Japan) was added to each well (Ding et al., 2005) and incubated for 4 h to allow the conversion of MTT to formazan crystals by mitochondrial dehydrogenase,

prior to the addition of 100 µl of 10 % (v/v) SDS in 50 % (v/v) N, N-dimethylformamide (Merck, USA) to solubilize the formazan crystals without removing the medium (Uma et al., 2008). An ELISA plate reader (Multiskan EX, Thermo Scientific, USA) was used to record the absorbance at 570 nm. The percentage of cell viability was calculated using following equation: % Cell viability = 100 - % Cytotoxicity (% Cytotoxicity = 1- (mean absorbance of treated cells/ mean absorbance of negative control)) (Valiyari et al., 2012).

The cytotoxic effect of rcPAP on this cell line was also determined by the Trypan blue viability assay (Billack et al., 2008). Cells (10^4 per well) in 24 well plates were cultured at similar concentrations of rcPAP (as described above) for 72 h. Then, the medium was removed from the wells, and the cells were washed with PBS. Cells were detached by adding 100 µL of 0.5 % Trypsin/EDTA (Invitrogen, USA). DMEM supplement with 10 % FBS (50 µL) and 0.5 % Trypan blue (50 µL) (Merck, USA) were added to each well, and the plates were incubated for 5 min. Then, a 20 µL aliquot was removed and placed on a Neubauer hemocytometer (Precicolor, Germany). Finally, the numbers of viable and nonviable cells were counted under a microscope. The percent viability was calculated as: (viable cells/ the total cell count) × 100.

Cell transduction assays of rcPAP

For determination of protein transduction efficiency, the rcPAP internalization was assessed by western blot analysis (Rider et al., 2011; Zhang et al., 2013). MARC-145 cells in 6-well plates were cultured in DMEM with rcPAP at a concentration of 40, 60, 80 and 120 μg/ml for varying times (up to 5 h) and then cells were trypsinized and washed thoroughly in PBS to remove any rcPAP on the cell surface (Zhang et al., 2013). The cells in a well of plate were washed three times with PBS and lysed in pre-cold lysis buffer (1% Triton X-100, 1 mM PMSF in PBS) for 10 min (Zhang et al., 2013). Lysates from approximately 10^5 cells were added to the well. A known amount of purified rcPAP was used as a standard as indicated. The rcPAP were identified using western blotting with mouse anti-6x His monoclonal antibodies (1: 1,000 dilution) (GenScript, USA) and goat anti-mouse IgG HRP (1: 2,000 dilution) (GenScript, USA).

To test rcPAP persistence inside the cells, four concentrations of rcPAP (as shown above) were administered to culture medium and incubated for 5 h and then cells were washed by PBS and putted into medium without rcPAP (Zhang et al., 2013). The cells were collected every 12 h (up to 72 h) and analysed as described above.

Antiviral activity of the rcPAP

The antiviral assay was performed in six independent experiments. The MARC-145 cells were seeded in a 6-well plates at a density of 10^5 cells per well and cultured for 24 h at 37 °C, in a 5 % CO_2 incubator. Then the cells were inoculated with Thai isolated US strain PRRS virus at a 200 $TCID_{50}$ per well for 6 h at 37 °C, and the viral inoculum was then removed and the cell monolayer was washed with PBS. The various concentrations of rcPAP (40, 60, 80, and 120 μg/ml) with fresh medium were added (Guo et al., 2015). One positive control (cell lines inoculated with virus without rcPAP) and two negative controls (one cell lines with medium only and another with rcPAP) were included. The cells were cultured for 24 hpi; 48 hpi or 72 hpi after each rcPAP administration to medium at 37 °C, in a 5 % CO_2 incubator, the supernatants was collected for virus yield titration. The quantitative real time RT-PCR (qRT-PCR) was tested the viral RNA in either culture cells or supernatants at different times post-inoculation. Viral titers in the culture supernatants were determined and calculated as log10 ($TCID_{50}$/ml). The monkey active caspase-3 levels (a key protease activated during early stages of apoptosis) in culture cells were determined using ELISA analysis (Wardi et al., 2014). Western blot technique was used to detect nucleocapsid (N) protein synthesis of PRRS virus in culture cells.

Quantitative Real-time RT-PCR (qRT-PCR)

The qRT-PCR was used to detect and quantify viral RNA copy numbers based on ORF7 gene of PRRS virus (Wernike et al., 2012; Guo et al., 2015). The positive pCR2.1-ORF7-US plasmid was constructed using a pCR2.1®TA cloning kit (Invitrogen, USA) according to the manufacturer's instruction. Viral RNA was extracted from either culture cells or supernatants. The procedure of total RNA isolation was performed following the protocol of commercial kit's instruction (PureLink™ Viral RNA/DNA Kit, Invitrogen, USA). Then, RNA concentration was measured (using Nanodrop ND-2000, Thermo Scientific, USA), diluted to equal concentration and reverse-transcribed onto cDNA by using Superscript® III Reverse Transcriptase (Invitrogen, USA). The generated cDNA was amplified by qRT-PCR using the following specific primers as shown in Table 8.

Table 8 Nucleotide sequences of the primers used for qRT-PCR in this study

Gene	Sense	Sequence (5' to 3')	GenBank accession number	Product size (bp)	Reference
ORF7 of US strain PPRS virus	+	GCAATTGTGTCTGTCGTC	GU454850	81	(Wernike et al., 2012)
	-	CTTATCCTCCCTGAATCT GAC			

The qRT-PCR was developed for detection of each virus using SYBR Green I fluorescent dye using Thunderbird®Sybr®qPCR Mix (Toyobo, Japan). The qRT-PCR

reaction was performed using the ABI 7300 System (Applied Biosystems, USA) in 96-well plates. The cycling conditions were shown in Table 9.

Table 9 The qRT-PCR condition program

		cDNA	ORF7 of PRRS virus US strain
1 cycle	Denaturation		95 °C (1 min)
40 cycles	Denaturation		95 °C (1 min)
	Annealing		57 °C (15 sec)
	Extension (data collection)		72 °C (45 sec)

The qRT-PCR was performed in triplicates using 10-fold serial dilutions of the positive pCR2.1-ORF7-US plasmid with concentration ranging from 10 to 10 log10 (copies/ml) as standard. Positive (cells infected virus without rcPAP) and two negative (one cells only and another cells plus rcPAP) controls were tested along with the unknown samples.

Viral Titration

Viral titers in culture supernatants of PRRS virus were determined by log10 ($TCID_{50}$/ml). Briefly, cells were seeded onto 96-well culture plates at a density of 10^4 cells per well and then incubated for 24 h to reach at least 80 % confluence before infection. The viral culture supernatants were 10-fold serially diluted, from 10^{-1} to 10^{-9} dilution, and 200 µl of each dilution were putted to each of six wells. MARC-145 cell lines were maintained with medium free virus served as a control. The cells were incubated at 37 °C

in an incubator containing 5 % CO_2 for 72 hpi. The inverted microscope was used to daily check cell cytopathic effect (CPE) and IPMA technique was used to determine PRRS virus titers (Tatsanakit et al., 2003). The log10 ($TCID_{50}$/ml) was calculated using the Reed–Muench method (Reed and Muench, 1938).

Western blot analysis

The N protein of PRRS virus was performed using western blot analysis as described elsewhere (Guo et al., 2015; Pan et al., 2015). Briefly, the lysates from the rcPAP treated PRRS virus-infected MARC-145 cells were separated by SDS-PAGE (12.5 % (w/v) resolving gel) and then transferred to a polyvinyl difluoride (PVDF) membrane (Pall Corporation, USA) in transfer buffer (20 mM Tris-HCl, 192 mM glycine, 0.1 % (w/v) SDS, 20 % (v/v) methanol, pH 8.3) using a semi-dry transfer unit (Amersham, USA) for 1.5 h. The membrane was blocked with 5 % (w/v) skim milk in PBS at 4 °C overnight and then incubated with 1: 2,000 dilution of anti-PRRS virus N monoclonal antibodies (Rural Technologies, USA) at 37 °C for 1 h, washed three times in PBS/0.5 % (v/v) Tween 20 (PBS-T), and then incubated with 1: 2,000 dilution of horseradish peroxidase (HRP)-conjugated goat anti-mouse IgG (Sigma, USA) at 37 °C for 1 h. After washing (as above), the color was developed by incubation with the 3, 3-diaminobenzidine (Dojindo, Japan) for 15–30 min and the color development was terminated by rinsing with distilled water.

Apoptosis assays

Monkey active caspase-3 (which cleaved at Asp175/Ser176) from lysates of monkey cell lines was detected and quantified by using the Monkey Active caspase-3 ELISA Kit (MyBio-Source, USA) in 96-well plates under manufactory's instruction (Wardi et al., 2014). After treating cells with rcPAP, floated and adherent MARC-145 cells were pelleted and washed in cold PBS and lysed with cell extraction buffer (Invitrogen, USA) (10 mM Tris, pH 7.4, 100 mM NaCl, 1 mM EDTA, 1 mM EGTA, 1 mM NaF, 20 mM $Na_4P_2O_7$, 2 mM Na_3VO_4, 1 % Triton X-100, 10 % glycerol, 0.1 % SDS, 0.5 % deoxycholate) and 1 mM PMSF and protease inhibitor cocktail (Invitrogen, USA). The lysates were centrifuged at 13,000 rpm for 10 min at 4 °C. The protein concentration of cell extract supernatants was determined as the total protein using a BCA protein assay kit (Pierce, USA) with bovine serum albumin (BSA) at 25–2,000 µg/ml as the reference standards. The cell extract supernatants were then used to determine the concentration of monkey active caspase-3 levels (Wardi et al., 2014). The OD of this colored product was measured at 450 nm with an ELISA Reader (Multiskan EX, Thermo Scientific, USA), and this OD is directly proportional to the concentration of monkey active caspase-3 present in the sample. The results (ng/mg protein) represented as monkey active caspase-3 levels (ng) per protein concentration of cell extract supernatants (mg).

Statistics analysis

All data were presented as means ± standard deviation (S.D.) from six independent experiments. Each experiment involved triplicate wells per concentration. Statistical analysis was performed with analysis of variance (ANOVA) (F test). A $p < 0.05$ was considered statistically significant.

Results

Cell viability

The cytotoxicity of rcPAP was determined using MTT and Trypan blue assays as shown in Figure 14. The rcPAP treated MARC-145 cell lines showed no cytotoxicity from 40 μg/ml to a concentration of 80 μg/ml (100 % of cell viability) using either MTT or Trypan blue assays. However, this rcPAP showed cytotoxicity at the concentration of 120 μg/ml. The percentage of cell viability by using MTT assay was decreased 1.5 ± 0.28 % and by using Trypan blue assay was decreased 4.3 ± 0.09 %.

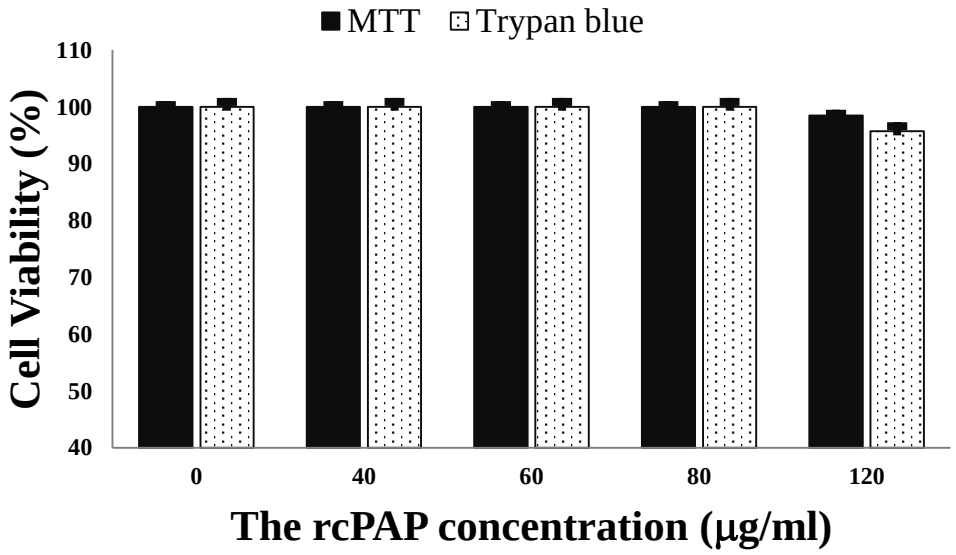

Figure 14. The cytotoxicity of the rcPAP in MARC-145 cells was measured using MTT and Trypan blue assay. Data are shown as mean ± SD of six independent experiments. Bars represent the standard deviation.

Cell transduction assay of rcPAP

The transduced rcPAP (35 kDa protein band) into MARC-145 cells was demonstrated by western blot analysis. Four concentrations of rcPAP (40, 60, 80 and 120 μg/ml) were examined its transduction and persistence on MARC-145 cell lines. The existed and persisted times of the rcPAP inside the MARC-145 cells were responded in a dose independent manner (data not shown). According to the reduction of percent cell viability of MARC-145 cells added with rcPAP at a concentration of 120 μg/ml, we designed to observe the effect of rcPAP at the 80 μg/ml. As shown in Figure 15, rcPAP bands were detected by using western blot technique in the MARC-145 cell lines, which treated with an 80 μg/ml. The results indicated that the rcPAP began to enter into MARC-145 cells within 1 h and still detected for a period of at least 72 h.

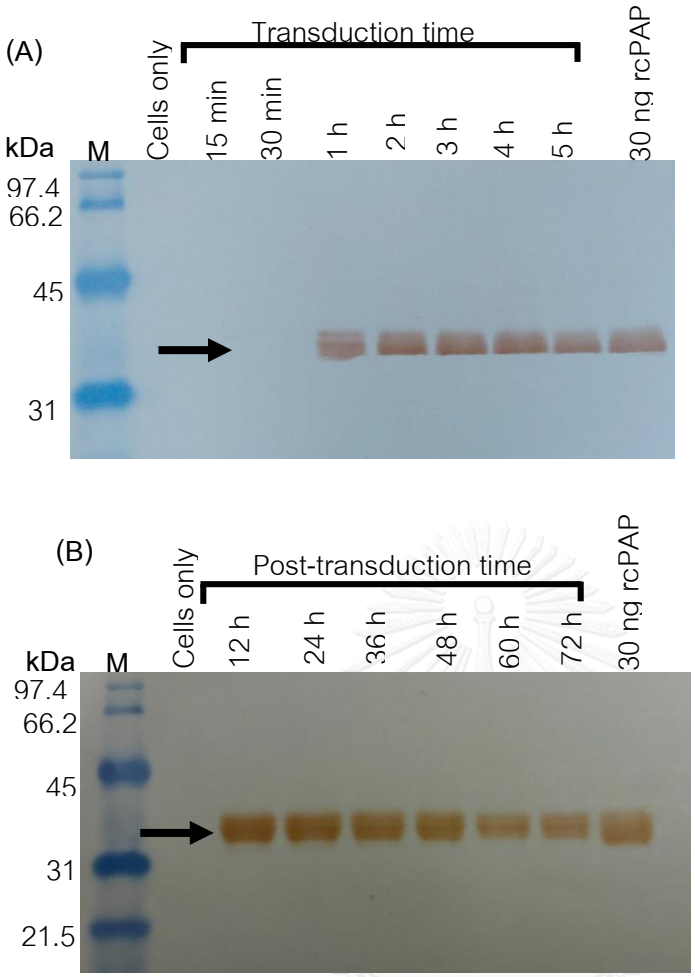

Figure 15. The product of rcPAP (80 μg/ml) transduced cells and persisted for days in MARC-145 cells. The western blot analysis of (A) transduction and (B) persistence of rcPAP. M, Protein markers (kDa); Protein markers (BioRad) were indicated in kDa.

Antiviral activity of the rcPAP

The qRT-PCR results showed that the rcPAP (40, 60, 80 and 120 μg/ml) significantly reduced PRRS viral copy numbers in a dose-dependent manner between rcPAP-treated and untreated PRRS virus-infected MARC-145 cells at three different periods (24, 48 and 72 h post inoculation (hpi)) ($p < 0.05$) as shown in Figure 16A and B.

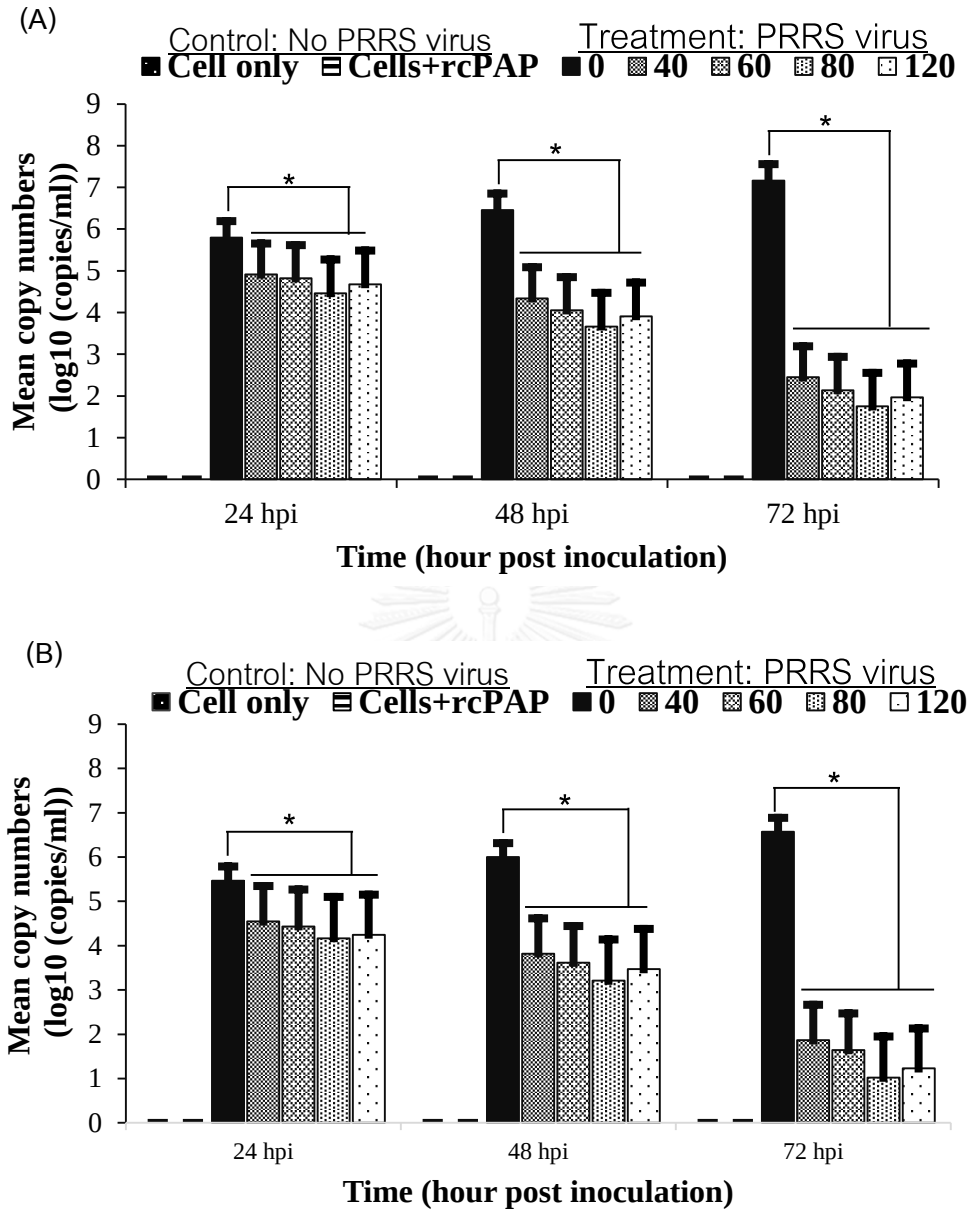

Figure 16. The enhanced antiviral effects of the rcPAP (μg/ml) treated PRRS virus infected MARC-145 cells at three time points in (A) culture cells and (B) culture supernatants were performed using qRT-PCR. Data are shown as mean ± SD of six independent experiments. Bars represent the standard deviation. The $p < 0.05$ (*).

As expected, the RNA copy numbers of two negative controls were undetermined in both culture cells and supernatants during the study. At 24 hpi, the highest reduction

of copy numbers of viral genome in rcPAP-treated PRRS virus-infected cells (80 μg/ml) was 23.1 % (4.46 ± 0.05 vs 5.8 ± 0.008 log10 (copies/ml)) in culture cells and 23.76 % (4.17 ± 0.05 vs 5.47 ± 0.01 log10 (copies/ml)) in culture supernatants compared with those of untreated MARC-145 cells. At 48 hpi following rcPAP (80 μg/ml) treated PRRS virus-infected MARC-145 cells, mean PRRS viral copy numbers (the highest reduction) were 43.18 % (3.67 ± 0.01 vs 6.46 ± 0.01 log10 (copies/ml)) in culture cells and 46.50 % (3.21 ± 0.003 vs 6.0 ± 0.008 log10 (copies/ml)) in culture supernatants compared with those of untreated MARC-145 cells. Interestingly, the rcPAP (80 μg/ml) treated PRRS virus-infected MARC-145 cells were significantly decreased the RNA viral copy numbers with the highest reduction by 75.55 % (1.75 ± 0.008 vs 7.16 ± 0.009 log10 (copies/ml)) in culture cells and 84.47 % (1.02 ± 0.002 vs 6.57 ± 0.02 log10 (copies/ml)) in culture supernatants at 72 hpi ($p < 0.05$). These results clearly showed that the highest reduction of viral copy numbers was found at a concentration of 80 μg/ml of rcPAP treated PRRS virus-infected MARC-145 cells. The inhibition of 80 μg/ml of rcPAP treated PRRS virus-infected MARC-145 cells at 72 hpi was taken pictures under the inverted microscope. As shown in Figure 17, the number of CPE (using IPMA technique) was dramatically lower in the rcPAP (80 μg/ml) treated infected MARC-145 cells (Figure 17B) compared with untreated control (Figure 17A) at 72 hpi. These results illustrated that the rcPAP had the antiviral activity *in vitro*.

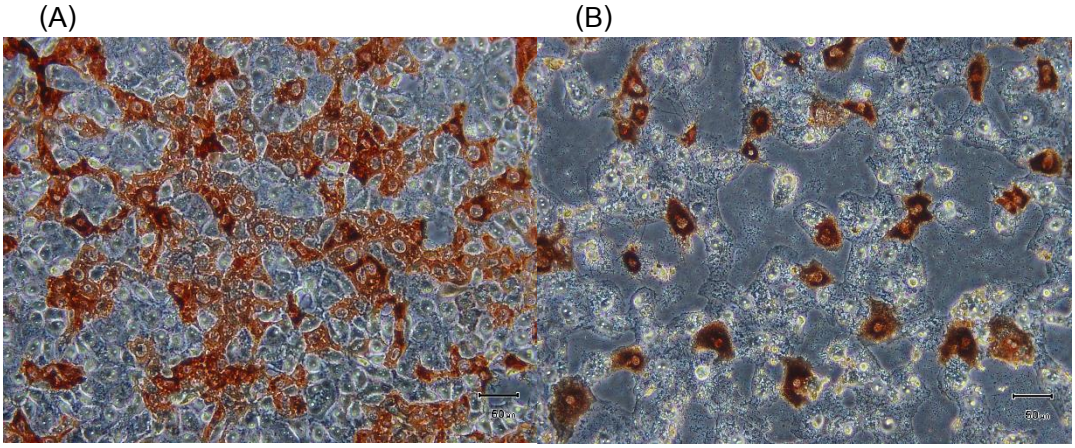

Figure 17. Inhibition of PRRS virus induced CPE in culture cells. The CPE was observed under microscopy. MARC-145 cells were infected with PRRS virus (200 $TCID_{50}$ per well) for 72 hpi. (A) PRRS virus infection without rcPAP and (B) PRRS virus infection with 80 μg/ml of rcPAP at 72 hpi.

In addition, the reduction of viral loads of the rcPAP against PRRS virus was determined. It showed that viral titers were significantly reduced in rcPAP (40, 60, 80 and 120 μg/ml) treated PRRS virus-infected MARC-145 cells ($p < 0.05$) at three different-time points (24, 48 and 72 hpi). As shown in Figure 18, the highest reduction of viral titers produced by the rcPAP-treated PRRS virus-infected MARC-145 cells at a concentration of 80 μg/ml compared with untreated PRRS virus-infected cells was 59.43 % (1.57 ± 0.005 vs 3.87 ± 0.01 log10 ($TCID_{50}$/ml)), 63.13 % (1.6 ± 0.006 vs 4.34 ± 0.01 log10 ($TCID_{50}$/ml)) and 87.76 % (0.63 ± 0.004 vs 5.15 ± 0.01 log10 ($TCID_{50}$/ml)) at 24, 48 and 72 hpi, respectively ($p < 0.05$). In this experiment, the results clearly demonstrated that rcPAP at a concentration of 80 μg/ml was significantly reduced by 87.76 % of PRRS virus titers at 72 hpi compared with untreated control ($p < 0.05$).

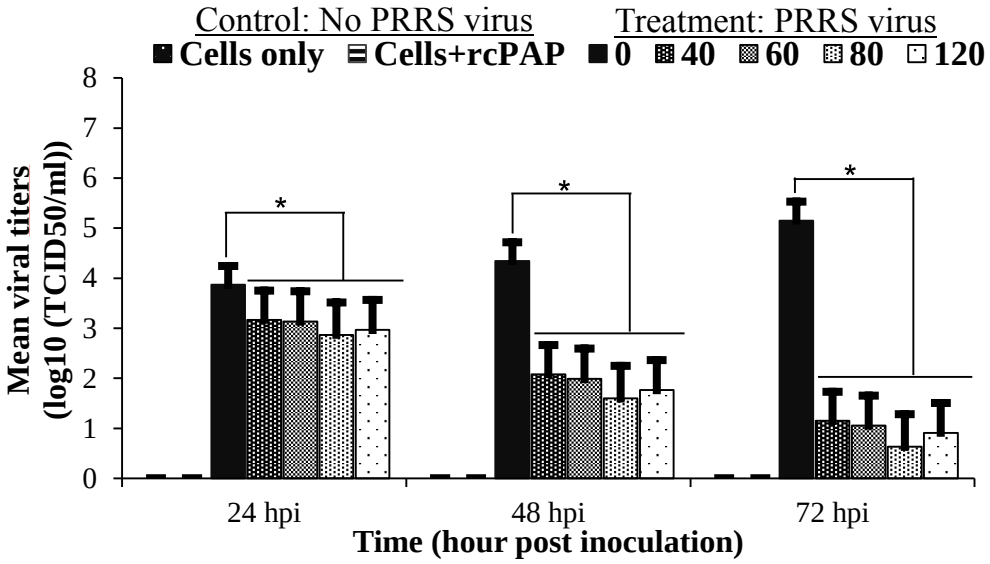

Figure 18. Mean viral titers in culture supernatants of the rcPAP (μg/ml) treated PRRS virus infected MARC-145 cells at three time points, respectively. Titers are expressed as log10 $TCID_{50}$ per ml of six independent experiments. Bars represent the standard deviation. The $p < 0.05$ (*).

The correlation between methods of qRT-PCR and viral titers in this study showed strong and positive linear relationship with r = 0.972 value as shown in Figure 19.

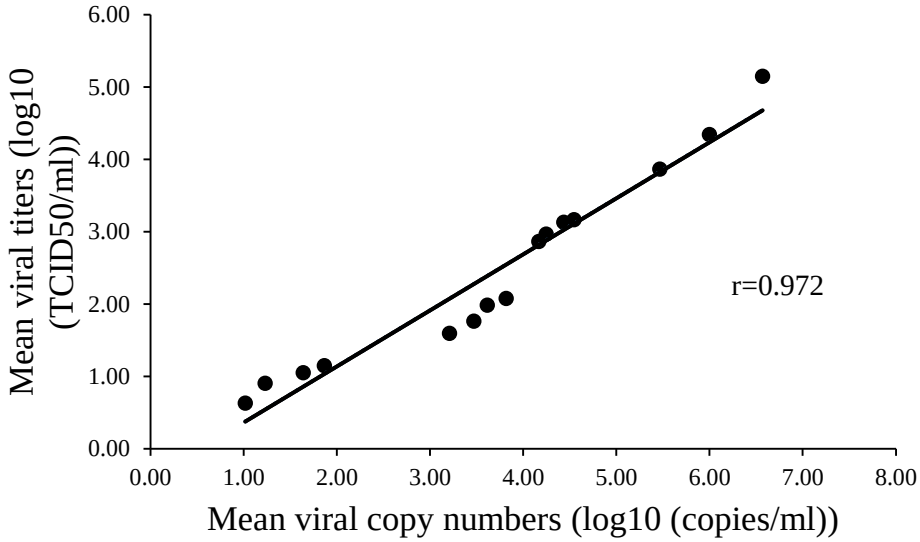

Figure 19. The correlation between methods of qRT-PCR (log10 (copies/ml) and viral titers (log10 ($TCID_{50}$/ml) in PRRS virus-infected MARC-145 cells.

To further validate the results obtained from qRT-PCR and viral titers, western blot analysis of virus-infected cell lines was detected the PRRS viral N protein band (15 kDa) at 24 hpi (Figure 20A) and 48 hpi (Figure 20B) but was not detected at 72 hpi (Figure 20C). Viral N protein synthesis was decreased when adding high concentration of rcPAP (80 and 120 μg/ml) in PRRS virus-infected MARC-145 cells at 48 hpi and was not detected at 72 hpi compared with untreated infected cells due to the reduction of viral propagation.

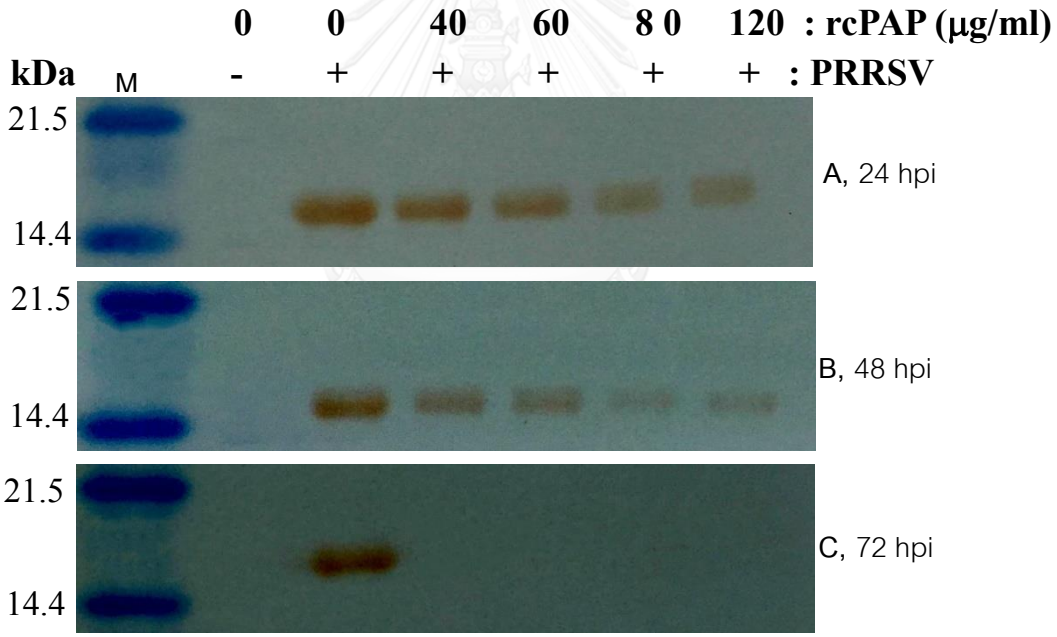

Figure 20. The band pattern of PRRS virus N protein was analyzed by western blot after treatment with the rcPAP (μg/ml) at the indicated concentrations or PBS for (A) 24 hpi, (B) 48 hpi and (C) 72 hpi, respectively. M, Protein markers. Protein markers (BioRad) on the gels are indicated in kDa.

Apoptosis assay

To examine the rcPAP induced apoptosis in PRRS virus-infected MARC-145 cells during the early phase of infection, monkey active caspase-3 levels were detected using ELISA analysis. As shown in Figure 21, the levels of monkey active caspase-3 in rcPAP (40, 60, 80 and 120 μg/ml) treated PRRS virus-infected MARC-145 cells were significantly increased in a dose-dependent manner compared to untreated PRRS virus-infected cells (positive control) at different-time points (24, 48 and 72 hpi) ($p < 0.05$). The results indicated that the highest monkey active caspase-3 levels in rcPAP (80 μg/ml) treated PRRS virus-infected MARC-145 cells were 12.69 fold (6.73 ± 0.008 vs 0.53 ± 0.003 (ng/mg protein)), 14.18 fold (9.08 ± 0.003 vs 0.64 ± 0.002 (ng/mg protein)) and 16.09 fold (13.36 ± 0.003 vs 0.84 ± 0.003 (ng/mg protein)) at 24, 48 and 72 hpi, respectively, compared with untreated control. From our results, the highest concentration of monkey active caspase-3 levels was 13.36 ng/mg protein at a concentration of 80 μg/ml of rcPAP treated PRRS virus-infected MARC-145 cells for 72 hpi. These data show that rcPAP has induced apoptosis in PRRS virus-infected MARC-145 cells.

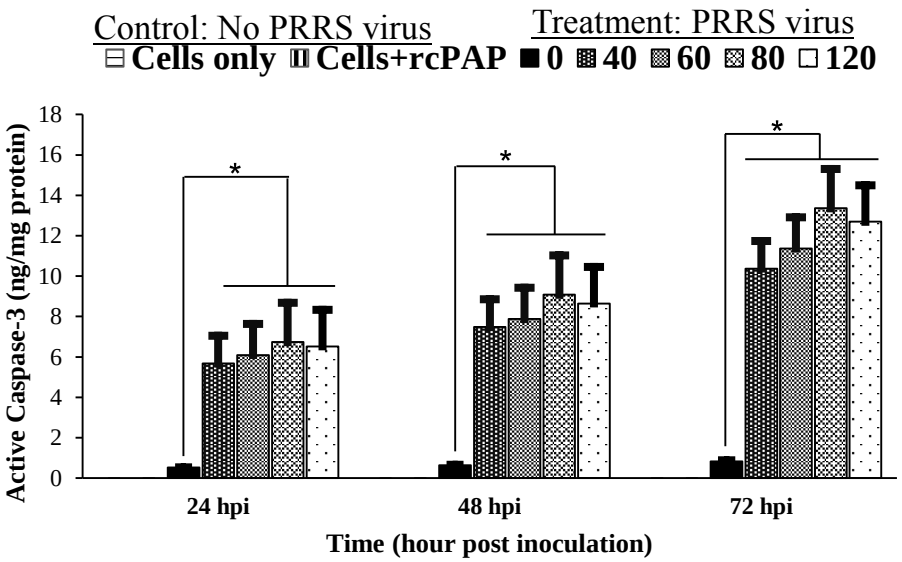

Figure 21. The monkey active caspase-3 levels in MARC-145 culture cells were measured via ELISA technique. Data are shown as mean ± SD of six independent experiments. Bars represent the standard deviation. The $p < 0.05$ (*).

Discussion

Human DRACO (Rider et al., 2011) and swine DRACO (Guo et al., 2015) have been reported to be used to control the viral diseases in vitro. These two pathways (interferon and apoptosis) originated from human DRACO concept can be combined to circumvent most viral blockades including PRRS virus as a major swine positive-strand RNA viruses (Rider et al., 2011; OIE, 2015). This study is the first report that rcPAP produced from bacteria, which is chimaeric protein, derived from swine PKR and swine Apaf-1 induced cell death and inhibited PRRS virus replication in MARC-145 cells. The antiviral effect of rcPAP appears to be more species specific. Not only the most of ideal antiviral molecules inhibit the synthesis of virus or stimulate host-encoded elements in controlling virus growth, but also our rcPAP can have biological effect to reduce the virus-infected cell lines as well. In this study, the HIV TAT domain as protein transduction domain (PTD) part was successfully fused with our rcPAP and showed the effect to deliver the rcPAP into MARC-145 cells as previously reported by Guo et al. (2015). TAT domain may be transduced rcPAP into MARC-145 cells via macropinocytosis as previously reported (Murriel and Dowdy, 2006). The transduction effect using western blot technique clearly demonstrated that the rcPAP got into and was inside MARC-145 cells and persisted for at least 3 days. Interestingly, the previous study by Rider et al. (2011) showed the persisted time of human DRACO molecule for at least 8 days. Further investigation needs to address the maximum times that rcPAP could persist inside the cells and still

have antiviral activity. We also found that the concentration of rcPAP at 40, 60 and 80 μg/ml is not toxic the normal cell lines by using MTT assay and Trypan blue assay. However, at a concentration of 120 μg/ml, rcPAP showed a few reductions of cell viability with less than 4.5 % with using both assays. Human DRACO molecule produced by bacteria (5 to 20 μg/ml) also had reported no toxicity in 11 studied cell lines (Rider et al., 2011). Comparing with swine DRACO produced by bacteria (Guo et al., 2015) at a concentration of 120 μg/ml showed very high cytotoxicity in reduction of cell viability more than 80 % in MARC-145 cell line. One explanation for this may be that the purified processes to reduce contaminated with *E. coli* toxin are important steps. Our purified rcPAP was used the specific purified column, dialyzed three times against PBS buffer overnight and confirmed single band protein (35 kDa) on membrane by using western blot analysis (Vo and Nuntaprasert, 2015, 2016). However, the observation of cytotoxicity of rcPAP on swine cell lines and primary cells origin and the reduction of bacterial toxin by using antitoxin absorbent column are need to be further study.

The dsRBD in dsRNA part of swine PKR in our rcPAP showed the effect on PRRS viral dsRNA detection because PRRS virus is belonged to the positive-strand RNA viruses (OIE, 2015). Weber et al., (2006) reported that the dsRNA in viral infected cells could be only detected with a positive-strand RNA, dsRNA, or DNA but not the negative-strand RNA virus (Weber et al., 2006). Similarly, the dsRBD detection of either human PKR in human DRACO or swine PKR in DRACO in swine are successfully bound to viral dsRNA

in virus-infected cells (Rider et al., 2011; Guo et al., 2015). The dsRBD of PKR of rcPAP may bind to PRRS viral dsRNA in interferon pathway (Dauber and Wolff, 2009).

Apoptosis is considered to be an important host defence mechanism that interrupts viral replication and eliminates virus-infected cells (Koyama et al., 2008). The CARD domain part in our rcPAP was constructed to induce apoptosis in virus-infected cells. The rcPAP molecule (80 μg/ml) was shown the significant effect to induce the apoptotic protein (active caspase-3) in MARC-145 cell line after PRRS virus infection at 72 hpi ($p < 0.05$). The monkey active caspase-3 levels were low concentration in virus-infected culture cells without rcPAP. As expected, the results of monkey active caspase-3 levels significantly increased 16.09 fold in PRRS virus-infected MARC-145 cells with rcPAP (80 μg/ml) at 72 hpi ($p < 0.05$). The studies of Rider et al. (2011) and Guo et al. (2015) have been demonstrated that the CARD domain of Apaf-1 induced apoptosis in virus-infected cells. In agreement with those studies, our rcPAP could induced apoptosis in PRRS virus-infected MARC-145 cells via activation of caspase 9 (caspase 9 is initiator caspase in intrinsic apoptotic pathway) (Elmore, 2007). Once activation, active caspase 9 activates caspase 3 (caspase 3 is the key protease activated during early apoptosis as apoptotic marker) (Elmore, 2007).

A time course study revealed that rcPAP showed the reduction of viral replication when it was added after the PRRS virus entered the cell line. Both validated methods from the correlation curve between the qRT-PCR and viral titers were confirmed and the

reduction of viral replication could be used in this study. The antiviral activity against PRRS virus-infected MARC-145 cells (200 $TCID_{50}$) clearly showed that rcPAP (concentration of 80 μg/ml) significantly reduced PRRS virus copy numbers (84.47 %) and viral titers (87.76 %) ($p < 0.05$) at 72 hpi. In comparison with previous reports by Liwei et al. (2015) using miRNAs and Li et al. (2015) using siRNAs highly showed the suppression of PRRS virus RNA copy numbers (about 40 %) and viral titers (about 60 %) by directly target to viral genome (Li et al., 2015; Liwei et al., 2015). In our knowledge, rcPAP did not destroy viral particles or directly inhibit viral replication by target viral genome instead of indirect via apoptotic induction to kill virus-infected cells. However, at a concentration of 120 μg/ml of rcPAP showed less antiviral activity than that of at 80 μg/ml. These results may be related to cytotoxicity of rcPAP. Although, the rcPAP was added to infected-cell line after viral inoculation, further study will be addressed at different administration time of rcPAP such as before or together with viral inoculation. The PRRS virus N protein, the most abundant viral protein expressed in infected cells, blocks host protein synthesis due to its high concentration in the nucleolus (Meulenberg, 2000; Suarez, 2000; Jourdan et al., 2012). Moreover, the PRRS virus N protein may affect transcriptional regulation in infected cells by interacting with transcriptional regulators (Dokland, 2010). Here, we showed that the rcPAP effectively decreased the synthesis of the viral N protein and CPE in PRRS virus-infected Marc-145 cells. Theoretically, our rcPAP did not directly inhibit viral protein synthesis. The reduction of viral N protein in rcPAP treated virus-infected cells may be

related to the apoptotic induction of rcPAP to kill virus-infected cells. It implies that rcPAP may reduce PRRS viral-infectious clones and viral loads. Taken together, rcPAP at the concentration of 80 μg/ml significantly showed the maximum enhanced antiviral activity (reduced viral copy numbers, viral titers, viral N protein and CPE by induction of apoptosis) in PRRS virus-infected cell lines at 72 hpi ($p < 0.05$). These results will address us to further investigate the in vivo effect of rcPAP on reduction of viral shedding in nursery pigs after vaccination with PRRS MLV vaccine.

In conclusion, the data included in this report provide that the rcPAP produced from bacterial system exhibits strong antiviral activity via apoptotic induction against PRRS virus in MARC-145 cell line. The rcPAP has potential to be used in the development of prophylactic and therapeutic strategies for this disease and other viral diseases in swine. However, the enhanced antiviral efficacy of the rcPAP need to further confirmation *in vivo*.

Conclusion

For application of the rcPAP to enhanced antiviral activity in swine diseases, the author carried out in this thesis on the basic research on the production of the rcPAP and its induction effect of apoptosis on MARC-145 cell line infected with US strain PRRS virus by the establishment of expression system, production, purification and biological activity analyses. The author first constructed the rcPAP, studied production of this protein and synthesized the mouse polyclonal antibodies against the rcPAP. Then, the enhanced antiviral activity against the US strain PRRS virus of the rcPAP was investigated in vitro.

In CHAPTER 1, the cloning step for construction and expression of rcPAP derived from US strain PRRS virus-infected PAM was carried out. The two expression plasmids were constructed, expressed and the expression levels were compared. The rcPAP gene in pET-His6-TEV-LIC plasmid could express as a soluble protein at a 2.4-fold higher concentration (12.32 mg purified rcPAP/l of culture) than that from the rcPAP gene in pQE32 plasmid at a low temperature (25 °C). In addition, the solubility test was performed under different temperatures and the optimal expression conditions (OD_{600} of 0.6, 0.75 mM of IPTG, at 25 °C and induction time for 18 h) for production of rcPAP were determined. Moreover, mouse polyclonal antibodies against rcPAP were produced and successfully reacted with purified rcPAP. The IFA pictures indicated that HIV TAT domain has been successfully delivered rcPAP into MARC-145 cell cytoplasm.

In CHAPTER 2, the author investigated the in vitro effects of the rcPAP molecule (at a concentration of 40, 60, 80 and 120 μg/ml) on Thai-isolated US strain PRRS virus-infected MARC-145 cells. Firstly, the cytotoxicity assay of rcPAP was examined on MARC-

145 cell line. The rcPAP at a concentration of 40, 60 and 80 μg/ml did not cause any toxicity to MARC-145 cells but at a concentration of 120 μg/ml was found 4.5 % of cytotoxicity. Secondly, the transduction and persistence time of rcPAP on MARC-145 cells were measured. The rcPAP was detected in intracellular MARC-145 cells at 1 h of inoculation and persisted in cells for at least 72 h. Thirdly, the effect of rcPAP was studied on MARC-145 cells after 6 h infected with US strain PRRS virus. The maximum concentration of rcPAP is 80 μg/ml and the significant enhanced antiviral activity was shown at 72 hpi ($p < 0.05$). The induction of cell death on US strain PRRS virus-infected MARC-145 cells with rcPAP treatment significantly increased the monkey active caspase-3 levels ($p < 0.05$). The significant reduction of viral copy numbers was observed in either culture cells or culture supernatants ($p < 0.05$). The viral titers of US strain PRRS virus was significantly decreased in rcPAP treated infected MARC-145 cells compared with untreated control. The N protein synthesis and CPE were also shown lower on the rcPAP treated US strain PRRS virus-infected cells than the untreated infected control.

The cloning, expression, production and purification of rcPAP and its enhanced antiviral activity *in vitro* in this thesis were performed. The obtained knowledge and tools here will contribute a lot not only on the basic research for recombinant chimeric protein production but also applied for improving antiviral protocol against swine infectious diseases.

REFERENCES

Abba, Y., Hassim, H., Hamzah, H., and Noordin, M. M. 2015. Antiviral Activity of Resveratrol against Human and Animal Viruses. Advances in Virology. 2015: 1-8.

Asano, A., Kon, Y., and Agui, T. 2004. The mRNA regulation of porcine double-stranded RNA activated protein kinase gene. J Vet Med Sci. 12: 1523-1528.

Bautista, E. M., Goyal, S. M., Yoon, I. J., Joo, H. S., and Collins, J. E. 1993. Comparison of porcine alveolar macrophages and CL 2621 for the detection of porcine reproductive and respiratory syndrome (PRRS) virus and anti-PRRS antibody. J Vet Diagn Invest. 5: 163-165.

Billack, B., Radkar, V., and Adiabouah, C. 2008. In vitro evaluation of the cytotoxic and antiproliferative properties of resveratrol and several of its analogs. Cell Mol Biol Lett. 13: 553-569. doi: 10.2478/s11658-008-0022-9

Boustanshenas, B., Bakhshi, B., Ghorbani, M., and Norouzian, D. 2013. Comparison of two recombinant systems for expression of cholera toxin B sununit from Vibrio cholerae. Indian J Med Microbiol. 31: 10-14.

Charerntantanakul, W. 2012. Porcine reproductive and respiratory syndrome virus vaccines: Immunogenicity, efficacy and safety aspects. World J Virol. 1: 23-30.

Cho, J. G., and Dee, S. A. 2006. Porcine reproductive and respiratory syndrome virus. Theriogenology. 66: 655-662.

Choi, H., Kim, J., Lee, C., Ahn, Y., Song, J., Baek, S., and Kwon, D. 2009. Antiviral activity of quercetin 7-rhamnoside against porcine epidemic diarrhea virus. Antiviral Research. 81: 77-81.

Costers, S., Lefebvre, D. J., Delputte, P. L., and Nauwynck, H. J. 2008. Porcine reproductive and respiratory syndrome virus modulates apoptosis during replication in alveolar macrophages. Arch. Virol. 153: 1453-1465.

Dauber, B., and Wolff, T. 2009. Activation of the Antiviral Kinase PKR and Viral Countermeasures. Viruses. 1: 523-544.

de Groot, N. S., and Ventura, S. 2006. Effect of temperature on protein quality in bacterial inclusion bodies. FEBS Lett. 580: 6471-6476.

Ding, X., Xu, F., Chen, H., Tesh, R. B., and Xiao, S. 2005. Apoptosis of Hepatocytes Caused by Punta Toro Virus (Bunyaviridae: Phlebovirus) and Its Implication for Phlebovirus Pathogenesis. Am J Pathol. 167: 1043-1049.

Dokland, T. 2010. The structural biology of PRRSV. Virus Res. 154: 86-97.

Dong, X. Y., Zhao, M. Q., Tang, S. Q., Wang, J. Y., Pei, J. J., Liu, W. J., Ju, C. M., Luo, Y. W., and Chen, J. D. 2012. Review of Different Strategies for Preventing and Controlling Classical Swine Fever. ISR J Vet Med. 67: 203-213.

Elmore, S. 2007. Apoptosis: A Review of Programmed Cell Death. Toxicol Pathol. 35: 495-516.

Francis, D. M., and Page, R. 2010. Strategies to optimize protein expression in E. coli. Curr Protoc Protein Sci. 24 21-29.

Govorkova, E. A., Ilyushina, N. A., McClaren, J. L., Naipospos, T. S., Douangngeun, B., and Webster, R. G. 2009. Susceptibility of highly pathogenic H5N1 influenza viruses to the neuraminidase inhibitor oseltamivir differs in vitro and in a mouse model. Antimicrob Agents Chemother. 53: 3088-3096.

Gump, J. M., and Dowdy, S. F. 2007. TAT transduction: the molecular mechanism and therapeutic prospects. Trends Mol Med. 13: 443-448.

Guo, C., Chen, L., Mo, D., Chen, Y., and Liu, X. 2015. DRACO inhibits porcine reproductive and respiratory syndrome virus replication in vitro. Arch Virol: 1-9.

Guo, C., Huang, Y., Cong, P., Liu, X., Chen, Y., and He, Z. 2014. Cecropin P1 inhibits porcine reproductive and respiratory syndrome virus by blocking attachment. BMC Microbiol. 14: 1-11.

Gupta, S. K., and Shukla, P. 2015. Advanced technologies for improved expression of recombinant proteins in bacteria: perspectives and applications. Crit Rev Biotechnol: 1-10. doi: DOI: 10.3109/07388551.2015.1084264

He, D., Zhang, X., Liu, K., Pang, R., Zhao, J., Zhou, B., and Chen, P. 2014. In vitro inhibition of the replication of classical swine fever virus by porcine Mx1 protein. Antiviral Research. 104: 128-135.

Heijbel, A. 2003. Purification of a protein tagged with (His)6 at its N-terminus, C-terminus, and both N- and C-termini using different metal ions. Life Science News. 15: 22-24.

Hu, Q., Wu, D., Chen, W., Yan, Z., Yan, C., He, T., Liang, Q., and Shi, Y. 2014 Molecular determinants of caspase-9 activation by the Apaf-1 apoptosome. PNAS. 111: 16254-16261.

Jeong, H., Song, Y., Lee, S., Lee, J., Park, S., Song, C., Ha, G., Oh, J., Oh, Y., and Choi, I. 2010. Comparative Measurement of Cell-Mediated Immune Responses of Swine to the M and N Proteins of Porcine Reproductive and Respiratory Syndrome Virus. Clin Vaccine Immunol. 17: 503-512.

Jourdan, S. S., Osorio, F. A., and Hiscox, J. A. 2012. Biophysical characterisation of the nucleocapsid protein from a highly pathogenic porcine reproductive and respiratory syndrome virus strain. Biochem Biophys Res Commun. 419: 137-141.

Karniychuk, U. U., and Nauwynck, H. J. 2013. Pathogenesis and prevention of placental and trans-placental porcine reproductive and respiratory syndrome virus infection. Vet Res. 44: 1-14.

Kim, H. S., Kwang, J., Yoon, J. J., Joo, H. S., and Frey, M. L. 1993. Enhanced replication of porcine reproductive and respiratory syndrome (PRRS) virus in a homogeneous subpopulation of MA-104 cell line. Arch Virol. 133: 477-483.

Kim, M., Park, H. S., Seo, K. H., Yang, H., Kim, S., and Choi, J. 2013. Complete Solubilization and Purification of Recombinant Human Growth Hormone Produced in Escherichia coli. PLoS One. 8: 1-8.

Koyama, S., Ishii, K. J., Coban, C., and Akira, S. 2008. Innate immune response to viral infection. Cytokine. 43: 336-341.

Li, L., Wei, Z., Zhou, Y., Gao, F., Jiang, Y., Yu, L., Zheng, H., Tong, W., Yang, S., Zheng, H., Shan, T., Liu, F., Xia, T., and Tong, G. 2015. Host miR-26a suppresses replication

of porcine reproductive and respiratory syndrome virus by upregulating type I interferons. Virus Res. 195: 86-94.

Li, Y., Wang, X., Bo, K., Wang, X., Tang, B., Yang, B., Jiang, W., and Jiang, P. 2007. Emergence of a highly pathogenic porcine reproductive and respiratory syndrome virus in the Mid-Eastern region of China. J Vet. 174: 577-584.

Liwei, L., Gao, F., Jiang, Y., Yu, L., Zhou, Y., Zheng, H., Tong, W., Yang, S., Xia, T., Qu, Z., and Tong, G. 2015. Cellular miR-130b inhibits replication of porcine reproductive and respiratory syndrome virus in vitro and in vivo. Sci Rep: 1-10. doi: 10.1038/srep17010

Ma, Z., Wang, Y., Zhao, H., Xu, A., Wang, Y., Tang, J., and Feng, W. 2013. Porcine Reproductive and Respiratory Syndrome Virus Nonstructural Protein 4 Induces Apoptosis Dependent on Its 3C-Like Serine Protease Activity. PLoS One. 8: 1-11.

MacroLab, Q. (2014). QB3 MacroLab LIC Expression Vectors: A Laboratory Manual (Vol. 8, pp. 1-31).

Meulenberg, J. J. 2000. PRRSV, the virus. Vet Res. 31: 11-21.

Meulenberg, J. J. M., Petersen den Besten, A., de Kluyver, E., van Nieuwstadt, A., Wensvoort, G., and Moormann, R. J. M. 1997. Molecular characterization of Lelystad virus. Vet. Microbiol. 55: 197-202.

Meurs, E., Chong, K., Galabru, J., Thomas, N. S. B., Kerr, L. M., Williams, B. R. G., and Hovanessian, A. G. 1990. Molecular Cloning and Characterization of the Human Double-Stranded RNA-Activated Protein Kinase Induced by Interferon. Cell. 62: 379-390.

Moghaddam, E., Teoh, B., Sam, S., Lani, R., Hassandarvish, P., Chik, Z., Yueh, A., Abubakar, S., and Zandi, K. 2014. Baicalin, a metabolite of baicalein with antiviral activity against dengue virus. Sci Rep: 1-8. doi: 10.1038/srep05452

Murriel, C. L., and Dowdy, S. F. 2006. Influence of protein transduction domains on intracellular delivery of macromolecules. Expert Opin Drug Deliv. 3: 1-8.

Nelsen, C. J., Murtaugh, M. P., and Faaber, K. S. 1998. Porcine Reproductive and Respiratory Syndrome Virus Comparison: Divergent Evolution on Two Continents. J Virol. 73: 270-280.

Neumann, E. J., Kliebenstein, J. B., Johnson, C. D., Mabry, J. W., Bush, E. J., Seitzinger, A. H., Green, A. L., and Zimmerman, J. J. 2005. Assessment of the economic impact of porcine reproductive and respiratory syndrome on swine production in the United States. J Am Vet Med Assoc. 227: 385-392.

Nguyen, M. T., Koo, B., Vu, T. T. T., Song1, J., Chong, S., Jeong, B., Ryu, H., Moh, S., and Choe, H. 2014. Prokaryotic Soluble Overexpression and Purification of Bioactive Human Growth Hormone by Fusion to Thioredoxin, Maltose Binding Protein, and Protein Disulfide Isomerase. PLoS ONE. 9: 1-10.

OIE. 2015. Porcine reproductive and respiratory syndrome. Terrestrial manual: 1-13.

Onodera, O., Roses, A. D., Tsuji, S., Vance, J. M., Strittmatter, W. J., and Burke, J. R. 1996. Toxicity of expanded polyglutamine-domain proteins in Escherichia coli. FEBS Letters. 399: 135-139.

Overend, C., Mitchell, R., He, D., Rompato, G., Grubman, M. J., and Garmendia, A. E. 2007. Recombinant swine beta interferon protects swine alveolar macrophages and MARC-145 cells from infection with Porcine reproductive and respiratory syndrome virus. J Gen Virol. 88: 925-931.

Pan, X., Kong, N., Shan, T., Zheng, H., Tong, W., Yang, S., Li, G., Zhou, E., and Ton, G. 2015. Monoclonal Antibody to N Protein of Porcine Epidemic Diarrhea Virus. Monoclon Antib Immunodiagn Immunother. 34: 51-54.

Pozzo, F. D., and Thiry, E. 2014. Antiviral chemotherapy in veterinary medicine: current applications and perspectives. Rev Sci Tech Off Int Epiz. 33: 1-27.

Quinn, P. J., Markey, B. K., Leonard, F. C., FitzPatrick, E. S., and Fanning, S. (2015). *Concise Review of Veterinary Microbiology* (W. Blackwell Ed. 2 ed.). Dublin.

Reed, L. J., and Muench, H. 1938. A simple method of estimating fifty percent endpoints. Am J Epidemiol. 27.

Rende-Fournier, R., Ortega, L. G., George, C. X., and Samuel, C. E. 1997. Interaction of the Human Protein Kinase PKR with the Mouse PKR Homolog Occurs via the NTerminal Region of PKR and Does Not Inactivate Autophosphorylation Activity of Mouse PKR. Virol J. 238: 410–423.

Reubold, T. F., Wohlgemuth, S., and Eschenburg, S. 2011. Crystal Structure of Full-Length Apaf-1: How the Death Signal Is Relayed in the Mitochondrial Pathway of Apoptosis. Cell. 19: 1074–1083.

Rider, T. H., Zook, C. E., Boettcher, T. L., Wick, S. T., Pancoast, J. S., and Zusman, B. D. 2011. Broad-Spectrum Antiviral Therapeutics. PLoS ONE. 6: 1-15.

Riedl, S. J., Li, W., Chao, Y., Schwarzenbacher, R., and Shi, Y. 2005. Structure of the apoptotic protease-activating factor 1 bound to ADP. Nature. 434: 926-933.

Riedl, S. J., and Salvesen, G. S. 2007. The apoptosome: signalling platform of cell death. NATURE REVIEWS. 8: 405-413.

Rosano, G. L., and Ceccarelli, E. A. 2014. Recombinant protein expression in Escherichiacoli: advance sand challenges. Front Microbiol. 5: 1-17.

Roy, A., Kucukural, A., and Zhang, Y. 2010. I-TASSER: a unified platform for automated protein structure and function prediction. Nat Protoc. 5: 725-738.

Samuel, C. E. 1993. The eIF-2 alpha protein kinase, regulators of translation in eukaryotes from yeasts to humans. J Biol Chem. 268: 7603-7606.

Sang, Y., Rowland, R. R., Hesse, R. A., and Blecha, F. 2010. Differential expression and activity of the porcine type I interferon family. Physiol Genomics. 42: 248-258.

Seo, H. W., Park, C., Han, K., and Chae, C. 2014. Effect of porcine circovirus type 2 (PCV2) vaccination on PCV2-viremic piglets after experimental PCV2 challenge. Vet Res. 45: 1-13.

Song, D., Moon, H., and Kang, B. 2015. Porcine epidemic diarrhea: a review of current epidemiology and available vaccines. Clin Exp Vaccine Res. 4: 166-176.

Sørensen, H. P., and Mortensen, K. K. 2005. Soluble expression of recombinant proteins in the cytoplasm of Escherichia coli. Microb Cell Fact. 4: 1-8.

Suarez, P. 2000. Ultrastructural pathogenesis of the PRRS virus. Vet Res 31: 47-55.

Sun, R. Q., Cai, R. J., Chen, Y. Q., Liang, P. S., Chen, D. K., and Song, C. X. 2012. Outbreak of porcine epidemic diarrhea in suckling piglets, China. Emerg Infect Dis. 18: 161-163.

Suryanarayana, N., Vanlalhmuaka, Mankere, B., Verma, Thavachelvam, K., and Tuteja, U. 2016. Soluble Expression and Characterization of Biologically Active Bacillus anthracis Protective Antigen in Escherichia coli. Mol Biol Int: 1-11.

Tatsanakit, A., Kesdangsakonwut, S., and Thanawongnuwech, R. 2003. Evaluation of monoclonal antibodies for PRRSV detection of the selected Thai isolated using immunoperoxidase monolayer assay (IPMA). 11th International Symposium of the World Association of Veterinary laboratory Diagnosticians and OIE seminar on biotechnology.

Tempesta, M., Camero, M., Bellacicco, A. L., Tarsitano, E., Crescenzo, G., Thiry, J., Martella, V., Decaro, N., Elia, G., Neyts, J., Thiry, E., and Buonavoglia, C. 2007. Potent inhibition of genital herpesvirus infection in goats by cidofovir. Antivir Ther. 12: 977-979.

Tian, Z. J., An, T. Q., Zhou, Y. J., Peng, J. M., Hu, S. P., Wei, T. C., Jiang, Y. F., Xiao, Y., and Tong, G. Z. 2009. An attenuated live vaccine based on highly pathogenic porcine reproductive and respiratory syndrome virus (HP-PRRSV) protects piglets against HP-PRRS. Vet. Microbiol. 138: 34-40.

Uma, S., Kelly, J. P., and Rajasekaran, S. K. 2008. An investigation of the value of the Tetrahymena pyriformis as a test organism for assessing the acute toxicity of antidepressants. Biomed Res. 19: 37-40.

Valiyari, S., Baradaran, B., Delazar, A., Pasdaran, A., and Zare, F. 2012. Dichloromethane and Methanol Extracts of Scrophularia oxysepala Induces Apoptosis in MCF-7 Human Breast Cancer Cells. Adv Pharm Bull. 2: 223-231.

Van Breedam, W., Verbeeck, M., Christiaens, I., Van Gorp, H., and Nauwynck, H. J. 2013. Porcine, murine and human sialoadhesin (Sn/ Siglec-1/CD169): portals for porcine reproductive and respiratory syndrome virus entry into target cells. Journal of General Virology. 94: 1955-1960.

Vlasova, A. N., Marthaler, D., Wang, Q., Culhane, M. R., Rossow, K., Rovira, A., Collins, J., and Jung, K. 2014. Distinct characteristics and complex evolution of PEDV strains, North America, May 2013-February 2014. Emerg Infect Dis. 20: 1620-1628.

Vo, T. P. V. A., and Nuntaprasert, A. 2016. Production of recombinant chimaeric swine PKR-APAF-1 proteins in a bacterial expression system. (Summitted Manuscript).

Vo, T. P. V. A., and Nuntaprasert, A. 2015. Production of recombinant chimeric swine PKR-Apaf1 proteins in E.coli from porcine alveolar macrophages (PAMs). Proceedings of the 7th Asian Pig Veterinary Society Congress. Manila, Philippine: O76.

Wardi, L., Alaaeddine, N., Raad, I., Sarkis, R., Serhal, R., Khalil, C., and Hilal, G. 2014. Glucose restriction decreases telomerase activity and enhances its inhibitor response on breast cancer cells: possible extra-telomerase role of BIBR 1532. Cancer Cell International. 60: 1-14.

Weber, F., Wagner, V., Rasmussen, S. B., Hartmann, R., and Paludan, S. R. 2006. Double-Stranded RNA Is Produced by Positive-Strand RNA Viruses and DNA Viruses but Not in Detectable Amounts by Negative-Strand RNA Viruses. J Virol. 80: 5059–5064.

Wensvoort, G., Terpstra, C., Pol, J. M., ter Laak, E. A., Bloemraad, M., de Kluyver, E. P., Kragten, C., van Buiten, L., den Besten, A., and Wagenaar, F. 1991. Mystery swine disease in The Netherlands: the isolation of Lelystad virus. Vet Q. 13: 121-130.

Wernike, K., Hoffmann, B., Dauber, M., Lange, E., Schirrmeier, H., and Beer, M. 2012. Detection and Typing of Highly Pathogenic Porcine Reproductive and Respiratory Syndrome Virus by Multiplex Real-Time RT-PCR. PLoS ONE. 7: 1-9.

Xiao, S., Wang, Q., Gao, J., Wang, L., He, Z., Mo, D., Liu, X., and Chen, Y. 2011. Inhibition of highly pathogenic PRRSV replication in MARC-145 cells by artificial microRNAs. J Virol. 8: 1-11.

Yang, Q., Gao, L., Si, J., Sun, Y., Liu, J., Cao, L., and Feng, W. 2013. Inhibition of porcine reproductive and respiratory syndrome virus replication by flavaspidic acid AB. Antiviral Research. 97: 66-73.

Zhang, X., He, D., Zhou, B., Pang, R., Liu, K., Zhao, J., and Chen, P. 2013. In vitro inhibition of vesicular stomatitis virus replication by purified porcine Mx1 protein fused to HIV-1 Tat protein transduction domain (PTD). Antiviral Research. 99: 149-157.

Zhao, C., Liu, S., Li, C., Yang, L., and Zu, Y. 2014. In Vitro Evaluation of the Antiviral Activity of the Synthetic Epigallocatechin Gallate Analog-Epigallocatechin Gallate (EGCG) Palmitate against Porcine Reproductive and Respiratory Syndrome Virus. Viruses. 6: 938-950.

Zhou, F., Zhao, J., Chen, L., Chang, H., Li, Y., Liu, H., Wang, C., and Yang, X. 2015. Complete Genome Sequence of a Novel Porcine Reproductive and Respiratory Syndrome Virus That Emerged in China. Genome Announc. 3: 1-2.

Zhou, P., Chou, J., Olea, R. S., Yuan, J., and Wagner, G. 1999. Solution structure of Apaf-1 CARD and its interaction with caspase-9 CARD: A structural basis for specific adaptor / caspase interaction. Proc Natl Acad Sci USA. 96: 11265-11270.

APPENDIX

APPENDIX A

Instrument and chemical substances

1. A -20°C refrigerator, Model SF-C997 (Sanyo, Thailand)
2. A -80°C refrigerator, Model 905 (Thermofisher Scientific, USA)
3. Centrifuge and Microcentrifuge
4. Experimental glasswares
5. Gel document system, Model GVM 20 (Synoptics, UK)
6. Gel electrophoresis system, Model GE-100 (Bioer technology Co. Ltd., China)
7. Heat block (Labnet International Inc., USA)
8. Incubator, Model BE-400 (Memmert Inc., Germany)
9. Lamina air flow, Model Bio II A (Telstar, Spain)
10. Micropipette (Labnet, USA) and Micropipette tips
11. PCR and protein assay

11.1 Agarose gel (Molecular grade)

11.2 1kb DNA marker

11.3 Prestain protein marker (Low range) (Bio-Rad, USA)

11.4 Ethidium bromide 10mg/ml (Sigma Aldrich Inc., USA)

11.5 Gel electrophoresis buffer (TAE) and protein running buffer

11.6 Loading dye (Fermantas, Canada) and Coomassie brilliant blue-R250 (CBB; Bio Basic, Canada)

11.7 SDS-PAGE gel (12.5% (w/v) acrylamide

11.8 Itaq DNA polymerase (iNtRon, South Korea) and Thunderbird®Sybr®qPCR Mix (Toyobo, Japan)

12. PCR cabinet (Biometra, Germany) and ABI 7300 System (Applied Biosystems, Foster City, CA)
13. PCR tube and Microcentrifuge tube
14. Vortex, Model K 550-GE (Scientific Inc., USA)
15. Shaking incubator, Model 311DS (Labnet International Inc., USA)

APPENDIX B

Physical map of plasmid pCR®-2.1 TA vector (Invitrogen, USA)

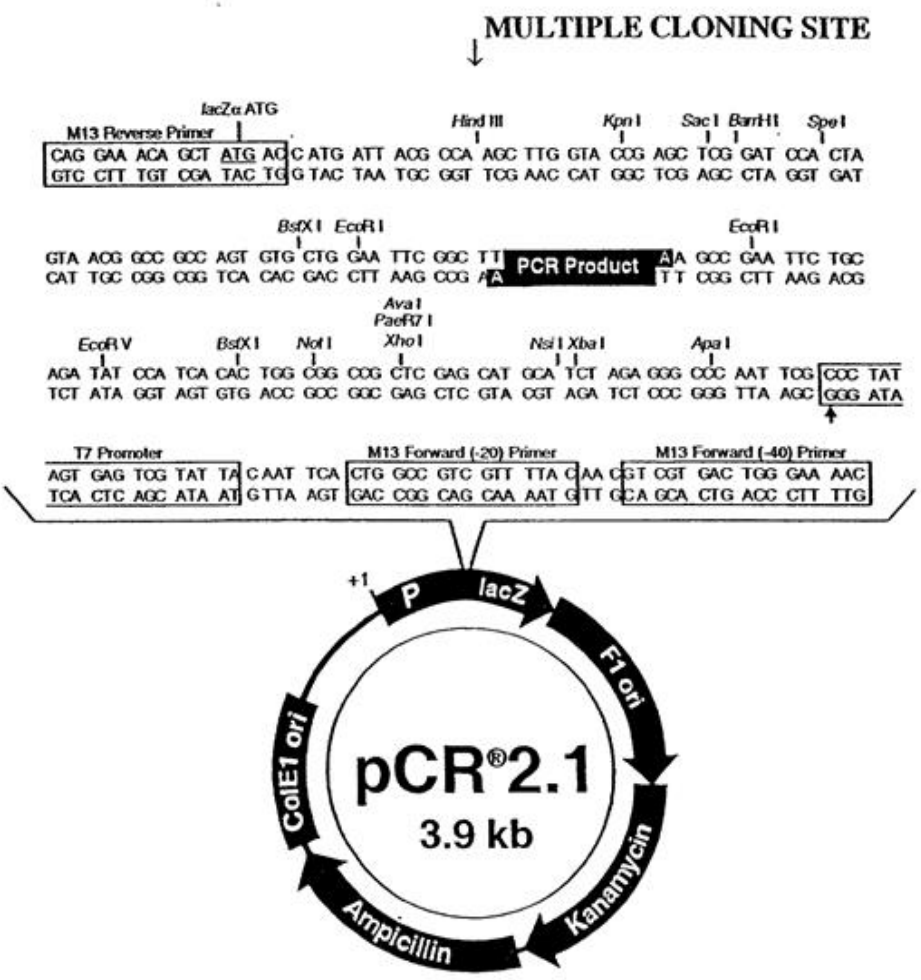

APPENDIX C

Physical map of plasmid pET His6 TEV LIC vector (Addgene, USA)

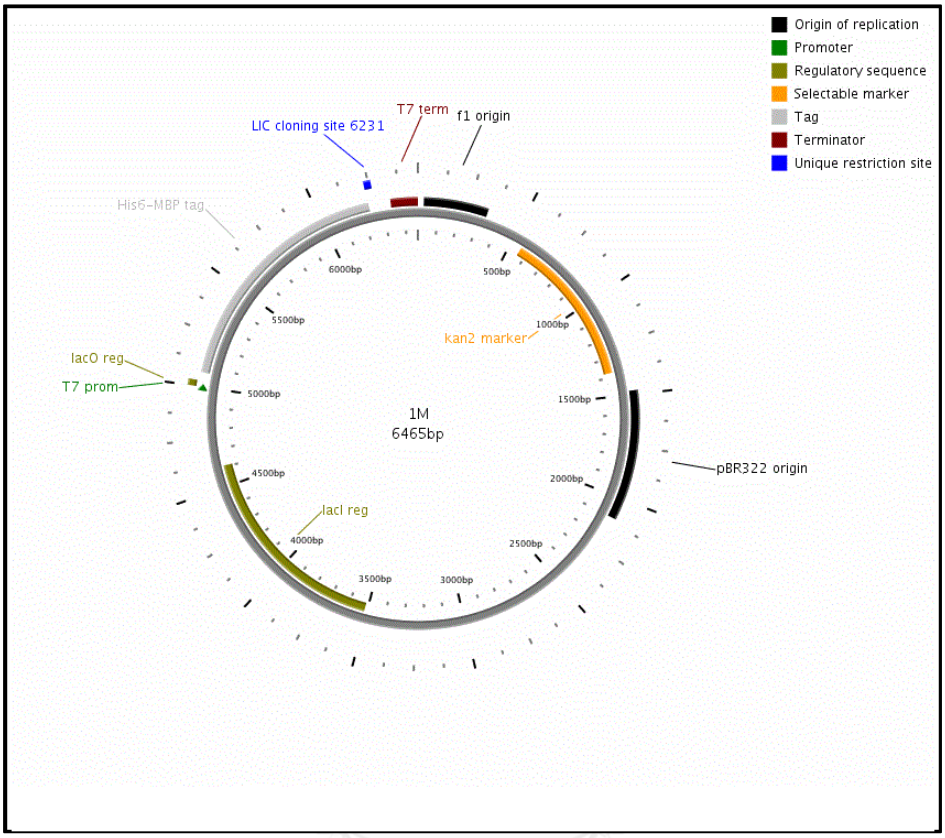

APPENDIX D

Physical map of plasmid pQE32 vector (QIAGEN, USA)

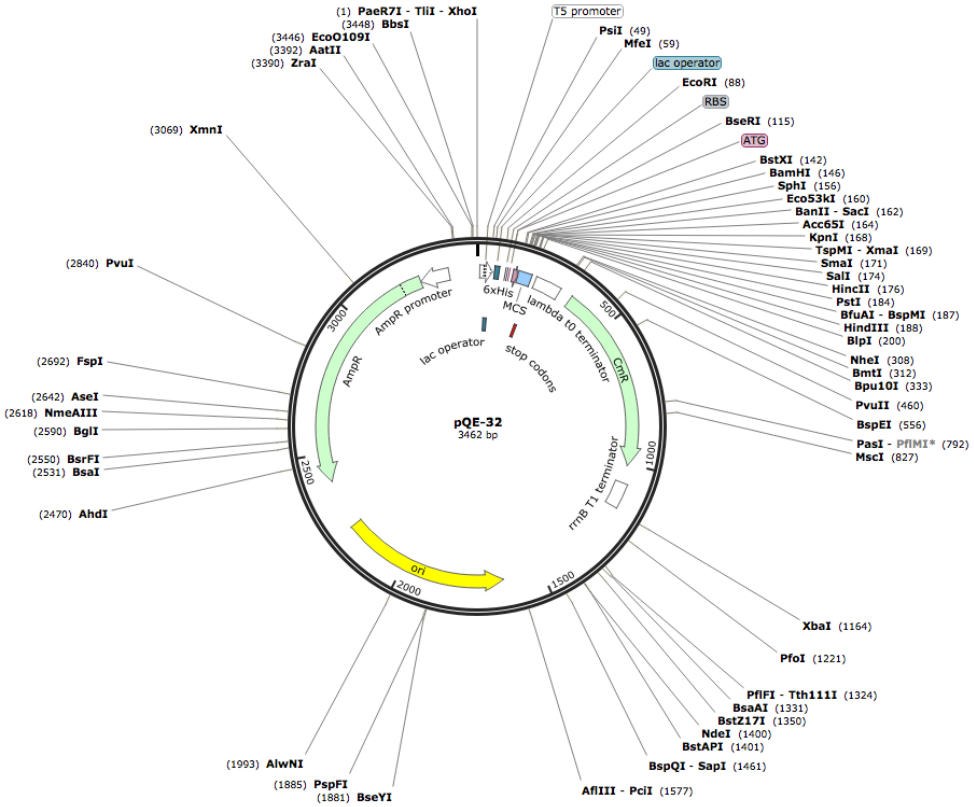

APPENDIX E

The statistical analysis of the qRT-PCR results in culture cells using ANOVA (as shown in Figure 16A)

Anova: Two-Factor With Replication

SUMMARY	24 hpi	48 hpi	72 hpi	Total
Cells only				
Count	6	6	6	18
Sum	0	0	0	0
Average	0	0	0	0
Variance	0	0	0	0
Cells+rcPAP				
Count	6	6	6	18
Sum	0	0	0	0
Average	0	0	0	0
Variance	0	0	0	0
Positive control				
Count	6	6	6	18
Sum	34.8	38.74	42.97	116.51
Average	5.8	6.456667	7.161667	6.472778
Variance	0.008	0.016067	0.009217	0.337127
40				
Count	6	6	6	18
Sum	29.47	26.05	14.69	70.21
Average	4.911667	4.341667	2.448333	3.900556
Variance	0.005657	0.004497	0.002097	1.177441
60				
Count	6	6	6	18
Sum	28.91	24.31	12.82	66.04
Average	4.818333	4.051667	2.136667	3.668889
Variance	0.015017	0.006697	0.005067	1.354505

80				
Count	6	6	6	18
Sum	26.78	21.99	10.5	59.27
Average	4.463333	3.665	1.75	3.292778
Variance	0.059387	0.01095	0.00896	1.39588
120				
Count	6	6	6	18
Sum	28.07	23.46	11.81	63.34
Average	4.678333	3.91	1.968333	3.518889
Variance	0.036217	0.00852	0.004817	1.391575
Total				
Count	42	42	42	
Sum	148.03	134.55	92.79	
Average	3.524524	3.203571	2.209286	
Variance	5.25902	4.957141	5.069929	

ANOVA

Source of Variation	*SS*	*df*	*MS*	*F*	*P-value*	*F crit*
Sample	570.0692	6	95.01154	9918.519	3.7E-142	2.186134
Columns	39.50052	2	19.75026	2061.785	5.46E-85	3.082852
Interaction	55.65463	12	4.637886	484.1618	4.88E-86	1.845515
Within	1.005817	105	0.009579			
Total	666.2302	125				

There are significant difference between rcPAP treatment and no treatment virus-infected MARC-145 cells at those rcPAP concentration at three different-time points.

APPENDIX F

The statistical analysis of the qRT-PCR results in culture supernatants using ANOVA (as shown in Figure 16B)

Anova: Two-Factor With Replication

SUMMARY	24 hpi	48 hpi	72 hpi	Total
Cells only				
Count	6	6	6	18
Sum	0	0	0	0
Average	0	0	0	0
Variance	0	0	0	0
Cells+rcPAP				
Count	6	6	6	18
Sum	0	0	0	0
Average	0	0	0	0
Variance	0	0	0	0
Positive control				
Count	6	6	6	18
Sum	32.8	36	39.41	108.21
Average	5.466667	6	6.568333	6.011667
Variance	0.018667	0.008	0.026017	0.229744
40				
Count	6	6	6	18
Sum	27.28	22.91	11.19	61.38
Average	4.546667	3.818333	1.865	3.41
Variance	0.017867	0.009697	0.00999	1.368376
60				
Count	6	6	6	18
Sum	26.61	21.68	9.84	58.13
Average	4.435	3.613333	1.64	3.229444
Variance	0.07011	0.001787	0.00264	1.478535

80				
Count	6	6	6	18
Sum	25	19.25	6.11	50.36
Average	4.166667	3.208333	1.018333	2.797778
Variance	0.005667	0.003137	0.002337	1.841689
120				
Count	6	6	6	18
Sum	25.47	20.82	7.37	53.66
Average	4.245	3.47	1.228333	2.981111
Variance	0.00223	0.00672	0.002337	1.735787
Total				
Count	42	42	42	
Sum	137.16	120.66	73.92	
Average	3.265714	2.872857	1.76	
Variance	4.54364	4.129967	4.420907	

ANOVA

Source of Variation	*SS*	*df*	*MS*	*F*	*P-value*	*F crit*
Sample	474.9943	6	79.16572	8880.77	1.2E-139	2.186134
Columns	51.23949	2	25.61974	2874.01	2.11E-92	3.082852
Interaction	60.94475	12	5.078729	569.7292	1.11E-89	1.845515
Within	0.936	105	0.008914			
Total	588.1146	125				

There are significant difference between rcPAP treatment and no treatment virus-infected MARC-145 cells at those rcPAP concentration at three different-time points.

APPENDIX G

The statistical analysis of the viral titers results in culture supernatants using ANOVA (as shown in Figure 18)

Anova: Two-Factor With Replication

SUMMARY	24 hpi	48 hpi	72 hpi	Total
Cells only				
Count	6	6	6	18
Sum	0	0	0	0
Average	0	0	0	0
Variance	0	0	0	0
Cells+rcPAP				
Count	6	6	6	18
Sum	0	0	0	0
Average	0	0	0	0
Variance	0	0	0	0
Positive control				
Count	6	6	6	18
Sum	23.2	26.06	30.91	80.17
Average	3.866667	4.343333	5.151667	4.453889
Variance	0.010667	0.018907	0.015217	0.311037
40				
Count	6	6	6	18
Sum	19	12.48	6.89	38.37
Average	3.166667	2.08	1.148333	2.131667
Variance	0.018667	0.0008	0.003377	0.727015
60				
Count	6	6	6	18
Sum	18.8	11.93	6.31	37.04
Average	3.133333	1.988333	1.051667	2.057778
Variance	0.002667	0.003057	0.004977	0.770407
80				
Count	6	6	6	18

Sum	17.2	9.59	3.79	30.58
Average	2.866667	1.598333	0.631667	1.698889
Variance	0.010667	0.006097	0.004417	0.893093
120				
Count	6	6	6	18
Sum	17.8	10.58	5.45	33.83
Average	2.966667	1.763333	0.908333	1.879444
Variance	0.002667	0.003427	0.004017	0.75777
Total				
Count	42	42	42	
Sum	96	70.64	53.35	
Average	2.285714	1.681905	1.270238	
Variance	2.236376	1.907372	2.768861	

ANOVA

Source of Variation	*SS*	*df*	*MS*	*F*	*P-value*	*F crit*
Sample	246.522	6	41.087	7870.833	6.8E-137	2.186134
Columns	21.91346	2	10.95673	2098.927	2.19E-85	3.082852
Interaction	36.34688	12	3.028907	580.2327	4.31E-90	1.845515
Within	0.548117	105	0.00522			
Total	305.3304	125				

There are significant difference between rcPAP treatment and no treatment virus-infected MARC-145 cells at those rcPAP concentration at three different-time points.

APPENDIX H

The statistical analysis of the monkey active caspase-3 levels in culture cells using ANOVA (as shown in Figure 20)

Anova: Two-Factor With Replication

SUMMARY	24 hpi	48 hpi	72 hpi	Total
Cells only				
Count	6	6	6	18
Sum	0	0	0	0
Average	0	0	0	0
Variance	0	0	0	0
Cells+rcPAP				
Count	6	6	6	18
Sum	0	0	0	0
Average	0	0	0	0
Variance	0	0	0	0
Positive control				
Count	6	6	6	18
Sum	3.2	3.86	5	12.06
Average	0.533333	0.643333	0.833333	0.67
Variance	0.003227	0.002747	0.003027	0.018906
40				
Count	6	6	6	18
Sum	34.04	44.9	62.22	141.16
Average	5.673333	7.483333	10.37	7.842222
Variance	0.001227	0.001067	0.0018	3.962101
60				
Count	6	6	6	18
Sum	36.54	47.24	68.21	151.99
Average	6.09	7.873333	11.36833	8.443889
Variance	0.00168	0.001867	0.004577	5.091343
80				
Count	6	6	6	18

Sum	40.39	54.49	80.17	175.05
Average	6.731667	9.081667	13.36167	9.725
Variance	0.008577	0.003777	0.003897	7.980991
120				
Count	6	6	6	18
Sum	39.12	51.86	76.14	167.12
Average	6.52	8.643333	12.69	9.284444
Variance	0.00536	0.005707	0.0048	6.940308
Total				
Count	42	42	42	
Sum	153.29	202.35	291.74	
Average	3.649762	4.817857	6.94619	
Variance	9.388739	16.55383	35.02079	

ANOVA

Source of Variation	*SS*	*df*	*MS*	*F*	*P-value*	*F crit*
Sample	2326.255	6	387.7092	152660.5	1.9E-204	2.186134
Columns	234.6497	2	117.3248	46196.65	2.5E-155	3.082852
Interaction	172.9757	12	14.41464	5675.765	9.4E-142	1.845515
Within	0.266667	105	0.00254			
Total	2734.147	125				

There are significant difference between rcPAP treatment and no treatment virus-infected MARC-145 cells at those rcPAP concentration at three different-time points.

VITA

Mr. Vo Phong Vu Anh Tuan was born on 19 September 1978 in Tiengiang province, Vietnam. He is Doctor of veterinary medicine, graduated from Faculty of Animal Science and Veterinary Medicine, Agriculture and Forestry University, Ho Chi Minh city, Vietnam in 2002. After graduation, he works as lecturer of major domesticated animal disease in Department of Veterinary Medicine, Faculty of Animal Husbandry and Veterinary Medicine, Southern Agriculture College, The Ministry of Agriculture and Rural Development. In 2012, he graduated Master degree in the field of veterinary medicine at Department of Veterinary Medicine, Faculty of Veterinary Science, Chulalongkorn University. In 2013, he applied and got the scholarship "Scholarship for International Graduate Students in ASEAN Countries'from Chulalongkorn University, Thailand during 2013-2016. He studied in the field of Veterinary Medicine at Department of Veterinary Medicine, Faculty of Veterinary Science, Chulalongkorn University.